UCRL 1856
cy 2

UNIVERSITY OF CALIFORNIA

Radiation Laboratory

TWO-WEEK LOAN COPY

This is a Library Circulating Copy which may be borrowed for two weeks. For a personal retention copy, call Tech. Info. Division, Ext. 5545

BERKELEY, CALIFORNIA

DISCLAIMER

This document was prepared as an account of work sponsored by the United States Government. While this document is believed to contain correct information, neither the United States Government nor any agency thereof, nor the Regents of the University of California, nor any of their employees, makes any warranty, express or implied, or assumes any legal responsibility for the accuracy, completeness, or usefulness of any information, apparatus, product, or process disclosed, or represents that its use would not infringe privately owned rights. Reference herein to any specific commercial product, process, or service by its trade name, trademark, manufacturer, or otherwise, does not necessarily constitute or imply its endorsement, recommendation, or favoring by the United States Government or any agency thereof, or the Regents of the University of California. The views and opinions of authors expressed herein do not necessarily state or reflect those of the United States Government or any agency thereof or the Regents of the University of California.

UCRL-1856
Unclassified-Physics Distribution

UNIVERSITY OF CALIFORNIA

Radiation Laboratory

Contract No. W-7405-eng-48

PHOTOPION PRODUCTION

Richard Madey

June 27, 1952

Berkeley, California

PHOTOPION PRODUCTION

Richard Madey

Radiation Laboratory, Department of Physics
University of California, Berkeley, California

June 27, 1952

ABSTRACT

Photopion production experiments are reviewed from an experimental point of view. The experimental results and their limitations are discussed for both charged and neutral pions.

PHOTOPION PRODUCTION

TABLE OF CONTENTS

I. INTRODUCTION

II. THE PHOTOPRODUCTION OF CHARGED PIONS

A. The Negative to Positive Ratio of the Production Cross Sections

1. Deuterium

a. The Experimental Evidence

1) Nuclear Emulsion Detection[2]

2) Double Focusing Magnet and Counters[3]

b. Physical Interpretation

2. The Z-Dependence of the Negative to Positive Ratio[3]

B. The Production of Positive Pions from Hydrogen[13]

1. The Experimental Technique

2. The Angular Distribution from 250 Mev Photons

3. The Energy Distribution at the Laboratory Angle of 90°

4. The Excitation Function

C. The Dependence of the Production Cross Sections on the Atomic Number Z and the Mass Number A

1. The Experimental Evidence

a. Electronic Identification of Positive Pions by Delayed Coincidences with Decay Electron[12].

b. Double Focusing Magnet and Counters[3]

2. The Physical Interpretation

III. THE PHOTOPRODUCTION OF NEUTRAL PIONS

A. The Gamma-Gamma Coincidence Detection Technique[16].

B. The Dependence of the Production Cross Section on the Mass Number A or Atomic Number Z

C. The Disintegration Kinematics of Neutral Pions

D. The Photoproduction of Neutral Pions from Beryllium

1. The Observed Angular Correlation

2. The Approximate Evaluation of the Energy Distribution of the Neutral Pions

3. The Absolute Cross Sections and the Angular Distribution of Neutral Pions from Beryllium

E. The Photoproduction of Neutral Pions from Hydrogen (Preliminary Data by Gamma-Gamma Coincidence Technique)

1. The Cross Sections

a. Polyethylene (CH_2) - Carbon Subtraction Method

b. Production from Liquid Hydrogen

2. The Excitation Function

F. The Photoproduction of Neutral Pions from Hydrogen[21] (by Pion-Proton Coincidences)

1. The Experimental Technique

2. The Excitation Function and the Cross Section

3. The Angular Distribution

PHOTOPION PRODUCTION

Richard Madey

Radiation Laboratory, Department of Physics
University of California, Berkeley, California

June 27, 1952

I. INTRODUCTION

The purpose of the following survey is to try to assess the contribution of photopion production experiments to our present knowledge of the nature of the pion field and of the character of the pion-nucleon coupling. This material was first presented in lecture form to members of the theoretical group at the Radiation Laboratory.

No direct cosmic ray experiments have been performed with photon produced pions; however, the production of pions by photons, which were generated by the Berkeley synchrotron, was definitely established in 1949 by McMillan and Peterson[1].

II. THE PHOTOPRODUCTION OF CHARGED PIONS

A. The Negative to Positive Ratio of the Production Cross Sections

1. Deuterium

a. The Experimental Evidence

1) Nuclear Emulsion Detection[2]

The nuclear emulsion data provides evidence that the negative to positive ratio from a D_2 gas target has a value close to unity and is relatively insensitive either to the energy or to the angle of production. The results are shown in Table 1.

TABLE 1 The Negative to Positive Ratio of Pions from Deuterium

Angle θ	E (Mev)	Ratio	Ratio (Alternate Method)
45°	43	0.79 ± 0.21	0.75 ± 0.22
	57	1.04 ± 0.16	1.15 ± 0.21
	87	0.89 ± 0.21	0.91 ± 0.24
	128	0.99 ± 0.30	0.73 ± 0.26
45° (Mean)		0.96 ± 0.10	0.94 ± 0.13
90°	34	1.24 ± 0.20	1.38 ± 0.32
	70	0.98 ± 0.14	1.08 ± 0.19
90° (Mean)		1.09 ± 0.12	1.20 ± 0.17
135°	39	1.37 ± 0.22	1.06 ± 0.20
	57	1.05 ± 0.18	1.13 ± 0.26
135° (Mean)		1.21 ± 0.17	1.08 ± 0.16
All Angles (Mean)		1.07 ± 0.07	1.04 ± 0.09

Results have been obtained at three production angles, viz. $\theta = 45^{\circ}{}^{+17^{\circ}}_{-15^{\circ}}$, $90^{\circ} \pm 16^{\circ}$, $135^{\circ} \pm 19^{\circ}$. The production angles were defined by channels lined with uranium. Data has been collected at four production energies for $\theta = 45^{\circ}$ and two production energies each at $\theta = 90^{\circ}$ and $\theta = 135^{\circ}$. The energies have been defined by means of absorbers. The errors shown are standard deviations due to statistics only.

2) Double Focusing Magnet and Counters[3]

Littauer and Walker[3] used a double focusing magnetic analyzer of Camac[4] to focus charged pions onto an array of counters. They found a π^-/π^+ ratio of 1.19 ± 0.12 for a pion energy of 65 ± 15 Mev and for a pion production angle of 135°. This value has been corrected for γ-ray absorption in the target. The time of flight of pions through the apparatus is of the order of one-half the mean life of the pions (or about 10^{-8} seconds).

b. The Physical Interpretation

1) To the approximation that the neutron-neutron forces are equal to the proton-proton forces, this experimental result is an argument that the nucleonic charge should not affect the photo-pion production process

except for determining the pionic charge.

2) Theoretical calculations have been made by Breuckner and Goldberger[6] and by Breuckner[7] of the negative to positive ratio for the photo pion production from free nucleons. If the interaction of the electromagnetic field of the photon is assumed to be only with the currents resulting from the charges of the moving protons and pions, then the calculation yields a ratio of the negative to the positive cross sections that depends both on the energy and the angle of pion production and that has values always greater than one.

The simple classical argument of Breuckner and Goldberger pointed out that there is an essential asymmetry in the production of negative and positive pions. When the negative pions are produced from neutrons, the charge-carrying nucleon is the final proton with large recoil velocity. When positive pions are produced, the proton is initially at rest and does not interact through its charge. Thus, if photopion production is assumed to take place according to the reactions $\gamma + n \rightarrow \pi^- + p$ and $\gamma + p \rightarrow \pi^+ + n$, and if a $(\vec{j} \cdot \vec{A})$ type interaction is assumed, where $\vec{j}$ = the current arising from a moving charge and $\vec{A}$ = the vector potential of the electromagnetic field, then the ratio of the production cross sections is

$$\frac{\sigma_{\pi^+}}{\sigma_{\pi^-}} = \left[\frac{(\vec{j} \cdot \vec{A})_{\pi^+}}{(\vec{j} \cdot \vec{A})_{\pi^-} + (\vec{j} \cdot \vec{A})_{\text{recoil } P}} \right]^2$$

Now, put $\vec{j} \cdot \vec{A} = \dfrac{e\vec{v} \cdot \vec{A}}{1 - \beta \cos \theta}$, and after some algebra, the result is

$\dfrac{\sigma_{\pi^+}}{\sigma_{\pi^-}} \doteq \left[1 - \dfrac{\mathcal{E}}{Mc^2} (1 - \beta \cos \theta) \right]^2 = F(T_\pi, \theta)$, where $\mathcal{E} = \mu_\pi + T$, M = nucleon rest mass, θ = pion production angle, and $v = \beta c$ = pion velocity.

Some typical values of this ratio for production at a laboratory angle of 90° are:

$$\frac{\sigma_{\pi^-}}{\sigma_{\pi^+}} = \begin{cases} 1.55 \text{ at } T_\pi = 40 \text{ Mev} \\ 1.83 \text{ at } T_\pi = 100 \text{ Mev} \end{cases}$$

[See Figure 1 of Breuckner, Phys. Rev. 79, 641 (1950) for detailed dependence of $\frac{\sigma_{\pi^-}}{\sigma_{\pi^+}}$ on θ and T_π.]

Effects of Coulomb field have been neglected; calculations show that Coulomb effect < 5 percent for $T_\pi = 30$ Mev.

Disagreement of this theory with experiment is possibly due to fact that assumption of negligible n-γ interaction is wrong, i.e. the interaction of the neutron through its magnetic moment with the electromagnetic field probably plays an important role in photo pion production. Indeed, if the photon interaction with the magnetic moment of the struck nucleon is the predominating interaction, then the resulting theoretical expression for the negative to positive ratio is essentially independent both of the energy and the angle of production. The ratio has a value near unity provided the numerical values of the anomalous magnetic moments, which are observed in a static field, are used. This assumption of the value of the anomalous moment observed in a static field is probably the weakest point of the argument.

Thus, the theory of the production process may be in agreement with the experimental results if the predominating interaction of the photon is with the magnetic moment rather than with the moving charges of the struck nucleons.

2. <u>The Z-dependence of π^-/π^+ Ratio</u>

Several investigators have contributed to our present knowledge of the π^-/π^+ ratio from light nuclei.

The π^-/π^+ ratio from <u>carbon</u> was found by McMillan, Peterson and White[8]

and by Peterson, Gilbert and White[8] to have a value near unity (≈ 1.3) and to be fairly independent of both the energy and angle of observation. These results were obtained with nuclear emulsion techniques. Jakobson[9] used the nuclear emulsion technique to measure the negative to positive ratio from ${}_2He^4$ at a production angle of 45°. His value of 0.99 ± 0.15 is integrated over the pion production energies.

The effect of nuclear structure on the negative to positive ratio is not easily interpretable quantitatively, because the pion-nucleon interaction may be different for the photo-production from a bound nucleon than from a free nucleon, and also because the nuclear interactions of the pions before leaving the nucleus have to be considered. If these two considerations are neglected for the photo-pion production from carbon, then the interpretation is the same as that for deuterium, namely that the predominant interaction of the photon is with the magnetic moments rather than with the moving charges of the struck nucleons.

Littauer and Walker[3] have obtained some interesting results for a production angle of 135° and a production energy of 65 ± 15 Mev[5]. An especially prominent deviation from a negative to positive ratio near unity was observed from the "double magic" ${}_{20}Ca^{40}$ nucleus.

The π^-/π^+ ratios of the symmetrical ($N = Z$) nuclei that they observed seem to fall on a smooth curve. They observed π^-/π^+ ratios from ${}_1H^2$, ${}_6C^{12}$, ${}_8O^{16}$, ${}_{16}S^{32}$, ${}_{20}Ca^{40}$ targets and obtained the following results:

Nucleus	π^-/π^+ per nucleus
${}_1H^2$	1.19 ± 0.12
${}_6C^{12}$	1.06 ± 0.02

Nucleus	π^-/π^+ per nucleus
$_8O^{16}$	1.04 ± 0.05
$_{16}S^{32}$	0.85 ± 0.03
$_{20}Ca^{40}$	0.58 ± 0.06

No stable symmetrical Nuclei exist with mass number A > 40

The π^-/π^+ ratios of the nuclei $_3Li^7$, $_4Be^9$, $_9F^{19}$, $_{13}Al^{27}$, $_{15}P^{31}$, $_{19}K^{39}$ each having one unpaired neutron were found to be

$_3Li^7$	2.06 ± 0.18
$_4Be^9$	2.25 ± 0.11 (cf. $_6C^{12}$ = 1.06 ± 0.02)
$_9F^{19}$	1.42 ± 0.05
$_{13}Al^{27}$	1.20 ± 0.05
$_{15}P^{31}$	1.04 ± 0.06
$_{19}K^{39}$	1.02 ± 0.1

The negative to positive ratios, measured by Littauer and Walker, are plotted in Figure 1 as a function of the mass number.

Machida and Tamura[10] obtained excellent agreement with the experimental results of Littauer and Walker for the negative to positive ratio from light nuclei. They assumed that pion production takes place from a tightly bound alpha cluster within the nucleus. The tight binding means that recoil energy is divided uniformly among all nucleons constituting the alpha cluster; therefore, in the final state, the probability of protons being in the nucleus will be reduced compared to that for neutrons by the effect of the coulomb potential barrier. This reduction of the probability for the final state is larger for negative pion production than for positive pion production because three protons and one neutron exist in the final state for negative pion production whereas three neutrons and one proton exist for positive pion production. Since the coulomb effect increases with atomic number

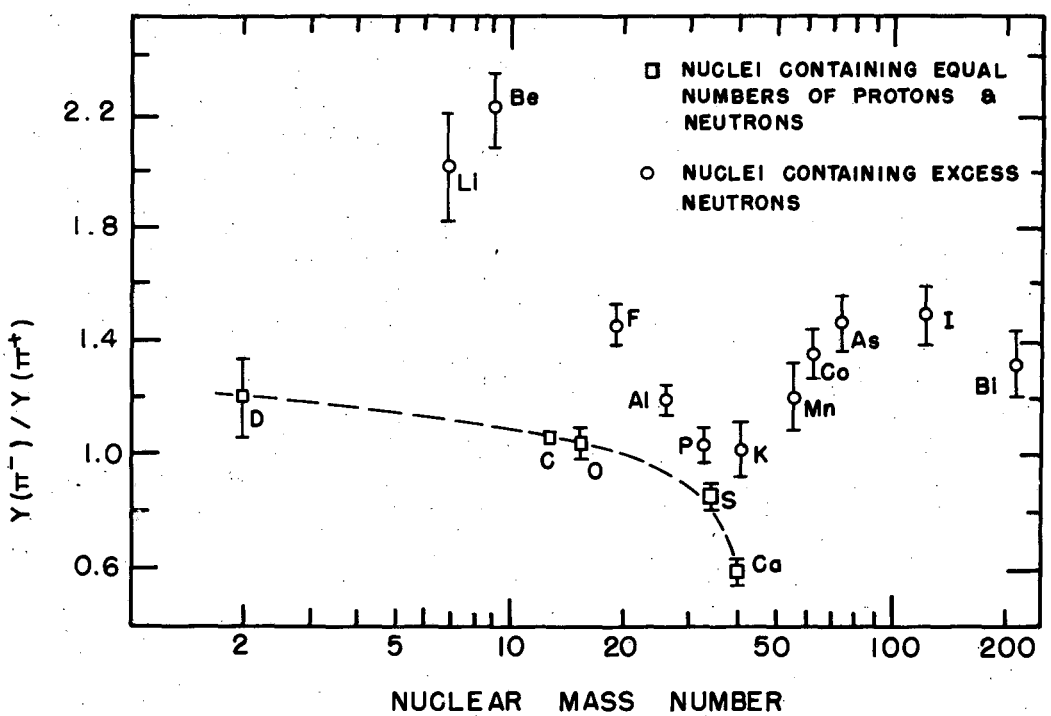
NUCLEI CONTAINING EQUAL NUMBERS OF PROTONS & NEUTRONS
NUCLEI CONTAINING EXCESS NEUTRONS
Y(π⁻) / Y(π⁺)
2.2
1.8
1.4
1.0
0.6
Be
Li
F
Al
D
C
O
P
K
S
Ca
Mn
Co
As
I
Bi
2
5
10
20
50
100
200
NUCLEAR MASS NUMBER

FIG. 1

MU3908

Z, the negative to positive ratio from the same type of nucleus (i.e. symmetrical or asymmertical) should decrease with Z. The asymmetrical nuclei were assumed to consist of a group of alpha clusters plus zero, one, or two neutrons of protons.

Littauer and Walker have presented an empirical correlation of the π^-/π^+ ratios with the mass differences $M_{Z-1} - M_{Z+1}$ of the masses of the ground states of the isobars adjacent in Z to the target nucleus. This correlation is illustrated in two plots: Figure 2 shows the π^-/π^+ ratios and the mass differences plotted against the atomic number, and Figure 3 shows the π^-/π^+ ratio plotted against the mass differences.

Medicus[10] applied nuclear emulsion detection to obtain the ratio $(\pi^-/\pi^+)_{Be^9} = 2.0 \pm 0.3$, at pion production energies $T_\pi = 40 - 70$ Mev and at the pion production angle $\theta = 90^\circ$.

Carothers[11] has measured the π^-/π^+ ratio from Be^9 as a function of production angle θ at a production energy $T_\pi \sim 54 \pm 16$ Mev by means of $B\rho$ and time of flight. He also measured this ratio from carbon at 90°. His results are

	θ	π^-/π^+ | $T_\pi \sim 54 \pm 16$ Mev
Be	60°	1.93 ± 0.12
	90°	1.96 ± 0.10
	150°	1.92 ± 0.11
C	90°	1.27 ± 0.07

The magnitude of the difference between π^-/π^+ ratios from C^{12} and from Be^9 cannot be explained merely by the higher neutron-proton ratio in the Be^9 nucleus. Instead, the high π^-/π^+ ratio from Be indicates that the very loose binding of the extra neutron in Be allows it to participate more actively in the production process than the other more tightly bound nucleons.

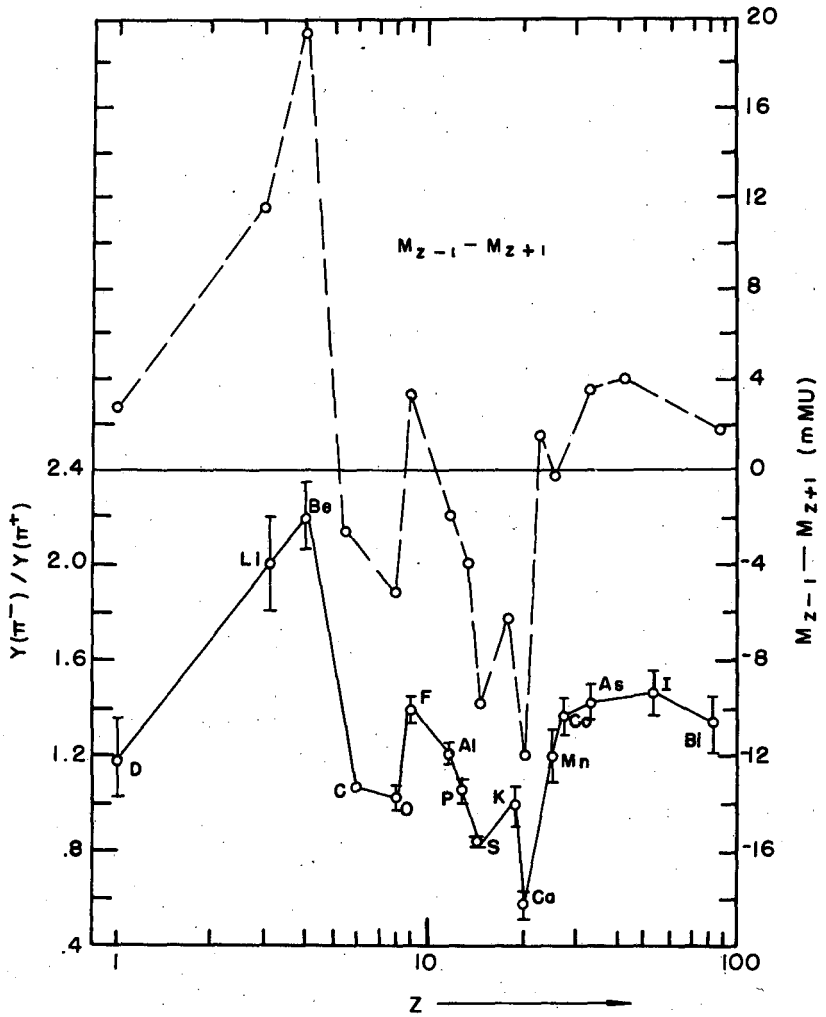
$M_{Z-1} - M_{Z+1}$
$Y(\pi^-)/Y(\pi^+)$
$M_{Z-1} - M_{Z+1}$ (mMU)
Z
D
Li
Be
C
O
F
Al
P
S
K
Ca
Mn
Co
As
I
Bi
20
16
12
8
4
0
-4
-8
-12
-16
2.4
2.0
1.6
1.2
.8
.4
1
10
100

FIG. 2 MU3909

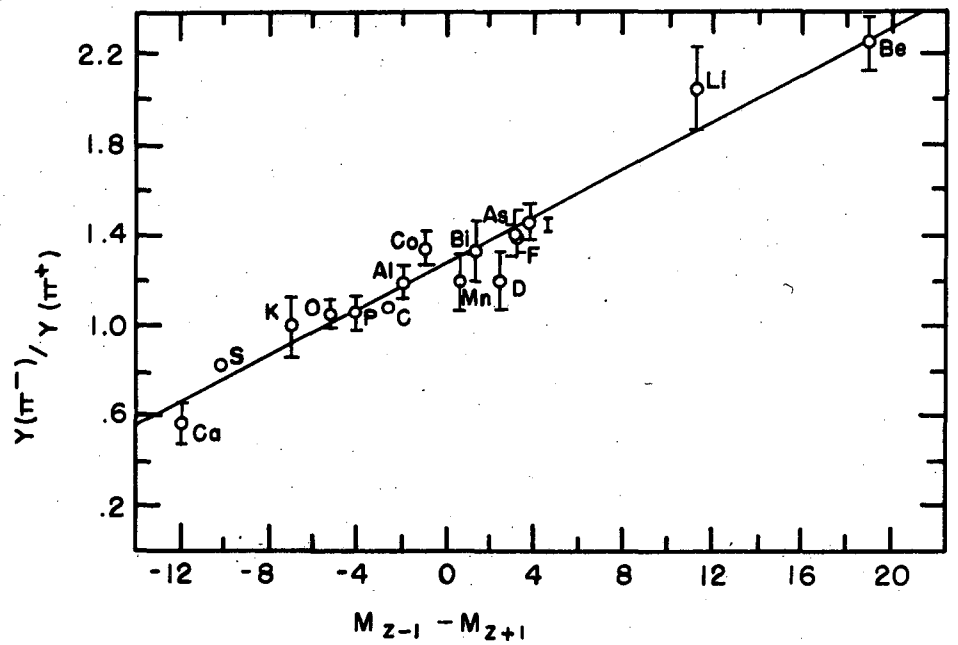
2.2
1.8
1.4
1.0
.6
.2
-12
-8
-4
0
4
8
12
16
20
$Y(\pi^-)/Y(\pi^+)$
$M_{Z-1} - M_{Z+1}$
Be
Li
As
I
Co
Bi
F
Al
Mn
D
K
O
P
C
S
Ca

FIG. 3 MU3910

For example, the ratio of the yield from an unpaired neutron to that from a paired neutron in Be^9 may be obtained from the measurements by using the following relationship.

$$\frac{\sigma_{\text{unpaired neutron}}}{\sigma_{\text{paired neutron}}} = 4\left[\frac{(\pi^-/\pi^+)_4 Be^9}{(\pi^-/\pi^+)_6 C^{12}} - 1\right]$$

The data of Littauer and Walker give a value of 4.5 ± 0.4 for this ratio at a production angle of 135°.

On the other hand, Carothers data at a 90° production angle gives the value 2.2 ± 0.5 for the ratio of the yields from an unpaired neutron and a paired neutron in Be^9; however, this ratio is quite sensitive to small changes in the measured values of the negative to positive ratios. The positive pion photoproduction data[13] at a production angle of 90° gives the value 2.3 ± 0.4 for the ratio of the positive pion yield from hydrogen to that from a bound proton in beryllium.

B. The Production of Positive Pions from Hydrogen[14]

1. The Experimental Technique

Steinberger and Bishop[14] identified positive pions with scintillation counters by requiring a delayed coincidence between the pulse generated when the positive pion stopped in the material of the phosphor and the subsequent pulse generated by the positron that resulted from the decay chain

$$\pi^+ \longrightarrow \mu^+ \ (T_{1/e} \cong 2.6 \times 10^{-8} \text{ sec})$$

$$\mu^+ \longrightarrow e^+ \ (T_{1/e} \cong 2.1 \times 10^{-6} \text{ sec})$$

The resolution of the electronic apparatus was insufficient to distinguish the separate pulses from the $\pi^+ \longrightarrow \mu^+$ part of the decay.

2. The Angular Distribution from 255 Mev Photons

The kinematical relationship $k = k(T, \theta)$, where $k \equiv$ the photon energy, $T \equiv$ the pion production kinetic energy, and $\theta \equiv$ the pion production angle, for the assumed tow-body reaction $\gamma + p \longrightarrow \pi^+ + n$ allows a measurement of the angular distribution of the pions that are produced by photons of a given energy by appropriately varying the absorber thickness at each angle to specify the pion production energy. In the Berkeley experiment, the meson range was chosen at the various angles so that the responsible incident photons had the energy 255 Mev in the laboratory system, or 204 Mev in the center of mass system.

Figure 4 shows the differential production cross section $d\sigma/d\Omega$ in cm^2 per steradian by 255 Mev photons versus the pion production angle in the center of mass coordinate system. This experimental curve has been described as being roughly isotropic, but perhaps with a slight peak in the backward direction. Now the angular distribution of a simple electric dipole effect varies according to the function $(\sin\theta/1 - \beta\cos\theta)^2$, where θ is the pion production angle and β is the pion velocity. This function is sharply peaked; the retardation factor in the denominator shifts the peak to the forward direction. Rather isotropic angular distributions are predicted by those theories in which the electromagnetic interaction is chiefly with the magnetic moment of the nucleons rather than with the electric charge of the pion.

3. The Energy Distribution at the Laboratory Angle of 90°

Pion production energies were selected by means of aluminum absorbers. Figures 5 and 6 show the spectral differential cross section

$$\frac{1}{Q}\left.\frac{d}{dT}\frac{d}{d\Omega}\right|_{\theta = 90^\circ}$$

in cm^2 per equivalent photon per Mev and per steradian at laboratory angle of 90° versus the pion production kinetic energy. A comparison of the results on a per nucleus basis for carbon and hydrogen shows that the cross section of six bound protons in ${}_6C^{12}$ is only about twice that

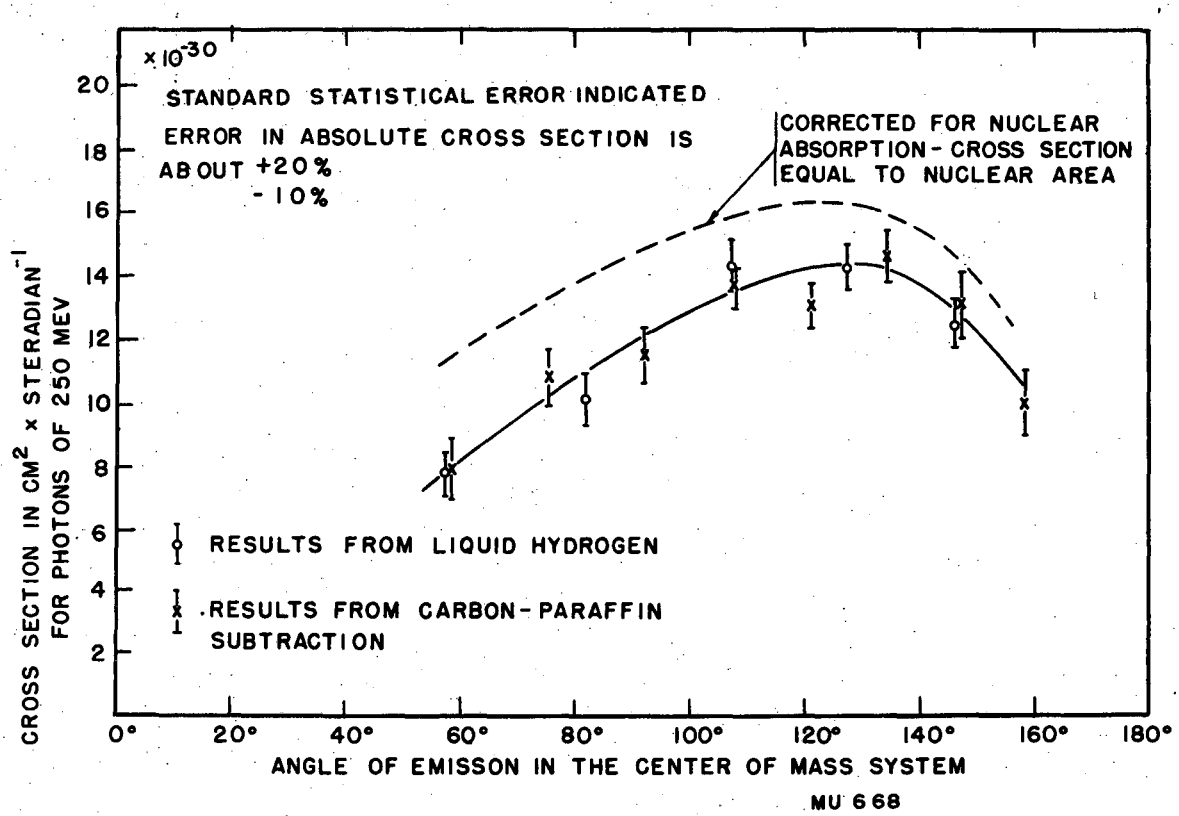
x 10^-30
STANDARD STATISTICAL ERROR INDICATED
ERROR IN ABSOLUTE CROSS SECTION IS
ABOUT +20%
-10%
CORRECTED FOR NUCLEAR
ABSORPTION - CROSS SECTION
EQUAL TO NUCLEAR AREA
RESULTS FROM LIQUID HYDROGEN
RESULTS FROM CARBON-PARAFFIN
SUBTRACTION
CROSS SECTION IN CM² x STERADIAN⁻¹
FOR PHOTONS OF 250 MEV
20
18
16
14
12
10
8
6
4
2
0°
20°
40°
60°
80°
100°
120°
140°
160°
180°
ANGLE OF EMISSON IN THE CENTER OF MASS SYSTEM
MU 668

Fig. 4

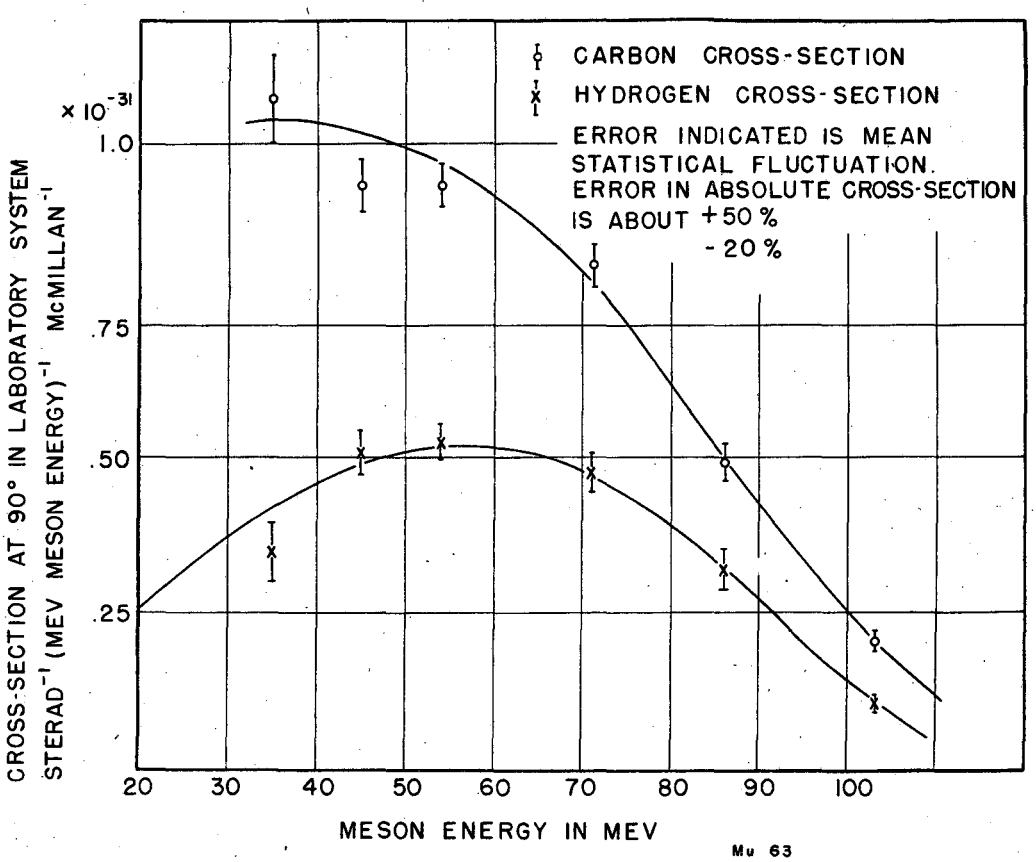
CARBON CROSS-SECTION
HYDROGEN CROSS-SECTION
ERROR INDICATED IS MEAN STATISTICAL FLUCTUATION.
ERROR IN ABSOLUTE CROSS-SECTION IS ABOUT +50 %
-20 %
x 10^-31
1.0
.75
.50
.25
CROSS-SECTION AT 90° IN LABORATORY SYSTEM
STERAD^-1 (MEV MESON ENERGY)^-1 McMILLAN^-1
20
30
40
50
60
70
80
90
100
MESON ENERGY IN MEV
Mu 63

Fig. 5

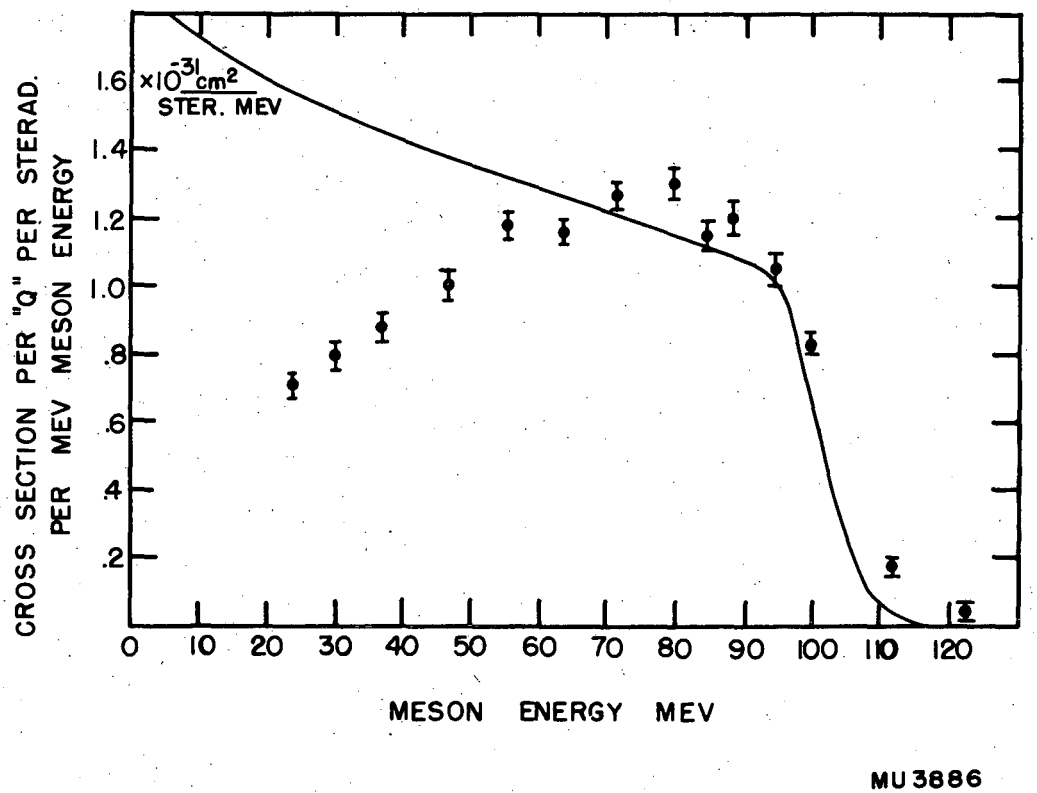
CROSS SECTION PER "Q" PER STERAD.
PER MEV MESON ENERGY
$\times 10^{-31}$ cm^2
STER. MEV
1.6
1.4
1.2
1.0
.8
.6
.4
.2
0
10
20
30
40
50
60
70
80
90
100
110
120
MESON ENERGY MEV
MU 3886

Fig. 6

of a single free proton. The inhibition of this reaction for the case of protons bound in nuclei is attributed[15] to the Pauli Exclusion Principle. The effect of the exclusion principle may be visualized qualitatively with the aid of the independent particle model (Fig. 7) of the carbon nucleus.

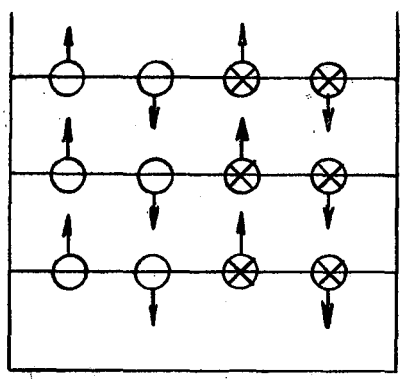

Fig. 7

Since the target proton changes its charge during the photoproduction process, the photon must transfer sufficient momentum to the target proton to elevate this nucleon to some higher energy state. Hence, very small momentum transfers are suppressed in the photo production of charged pions from nucleons bound in nuclei. This same result is usually expressed by saying that the volume available in the phase space of the residual nucleon is greater for a free proton than for a bound proton.

4. The Excitation Function

The excitation function of the differential cross section is derived from the energy distribution data. Let the photon spectrum I(k) be normalized so that

$$\int_0^{k_{max}} I(k)\, k\, dk = k_{max}\, Q$$

where Q is the number of "equivalent" photons[16] incident on the target. Then

$$\frac{d\sigma(k)}{d\Omega} = \left[\frac{\left(\frac{1}{Q}\frac{d^2 N}{d\Omega\, dT_\pi}\right)}{\left(\frac{I(k)}{Q}\right)}\right] \frac{dT_\pi}{dk}$$

where $\frac{1}{Q}\frac{d^2N}{d\Omega dT_\pi}$ is the number of pions per steradian per unit pion energy per "equivalent" photon and per target atom, and where the derivative dT_π/dk relates the produced pion energy interval to the producing photon energy interval. It is computed from the conservation laws for the two body process.

Figure 8 shows the differential cross section in cm^2 per steradian at a laboratory pion angle of 90° as a function of photon energy for photon energies in the interval from about 190 Mev to about 310 Mev. This curve is uncorrected for nuclear absorption of the pions. Note that the cross section rises approximately linearly to a plateau which starts at photon energies of about 260 Mev, the magnitude increases roughly by a factor of two from its value at a photon energy of 190 Mev to its value at a photon energy of about 260 Mev.

C. Dependence of the Production Cross Sections on the Atomic Number Z and the Mass Number A

1. The Experimental Evidence

a. Electronic Identification of π^+ by Delayed Coincidences with Decay Electrons[12]

Mozley[12] employed the Steinberger-Bishop electronic method of positive pion detection to measure the dependence on the atomic number of the production cross section at the production energies of 42 ± 7 Mev and 76 ± 6 Mev at the production angle of $90 \pm 8^\circ$. The experimental result, illustrated in Table 2, is that the yield per proton decreases with increasing atomic number.

TABLE 2

Element	42 Mev	Standard deviation (percent)	76 Mev	Standard deviation (percent)
H	6.6	17	8.07	11
Li	3.32	10	2.80	11
Be	2.82	11	2.13	10
B	3.02	11	2.28	15
C	2.60	6	1.93	5
Al	2.50	11	1.68	9
Cu	1.92	19	1.17	15
Sn	1.66	25	0.51	55
Pb	0.51	91	0.80	65

Identical shaped targets of approximately 1.5 g/cm^2 were used except for the tin and lead targets, which were about 1/10 the range; consequently, target thickness corrections of about 10 percent were required for the tin and lead points. The other corrections required for pion range, γ-ray absorption, impurities, and decay of pions in flight were of the order of 2 percent or less in most cases. No correction was made for nuclear absorption of the pions in

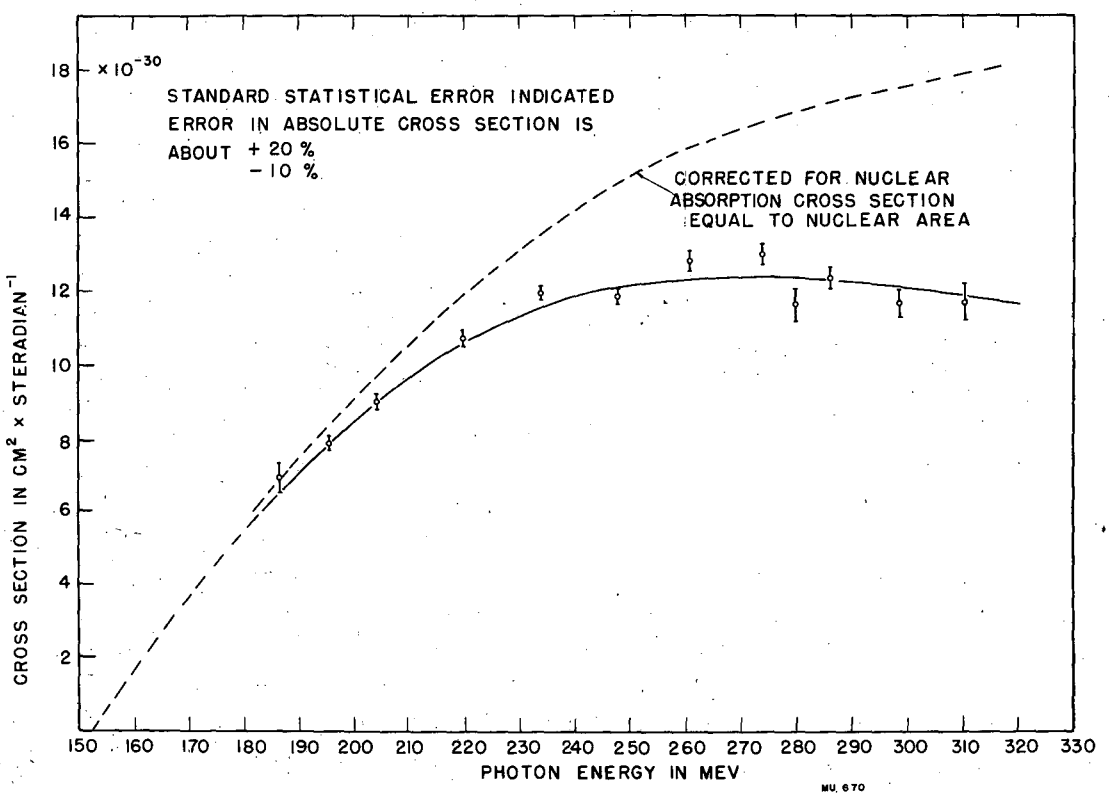
× 10^-30
STANDARD STATISTICAL ERROR INDICATED
ERROR IN ABSOLUTE CROSS SECTION IS
ABOUT + 20 %
− 10 %
CORRECTED FOR NUCLEAR
ABSORPTION CROSS SECTION
EQUAL TO NUCLEAR AREA
CROSS SECTION IN CM² × STERADIAN⁻¹
18
16
14
12
10
8
6
4
2
150 160 170 180 190 200 210 220 230 240 250 260 270 280 290 300 310 320 330
PHOTON ENERGY IN MEV
MU. 670

Fig. 8

the material of the absorbers. The hydrogen cross section was obtained by means of a polyethylene-carbon subtraction.

The number of positive pions produced per nucleon in the target may be fitted approximately by an $A^{-1/3}$ curve, where A is the mass number of the target nucleus. These data are not incompatible with the possibility that only the nucleons on the surface of the nucleus take part in photo-pion production.

b. Double Focusing Magnet and Counters[3]

Littauer and Walker[3] measured the yield of both positive and negative pions at a production angle of 135° and at a production energy of 65 ± 15 Mev from several target elements. The results are given in Table 2.

TABLE 3

Element	A	Z	Y (π^+)	Y (π^-)	Y (π^+) + Y (π^-)	Y (π^-)/Y (π^+)
H	1	1	1.00 ± 0.05	0.04 ± 0.05	1.04 ± 0.07	-
D	2	1	0.87 ± 0.07	1.04 ± 0.07	1.91 ± 0.10	1.19 ± 0.12
Li	7	3	2.25 ± 0.14	4.65 ± 0.28	6.90 ± 0.31	2.06 ± 0.18
Be	9	4	2.39 ± 0.01	5.39 ± 0.02	7.78 ± 0.03	2.25 ± 0.11
C	12	6	3.54 ± 0.05	3.77 ± 0.06	7.31 ± 0.08	1.06 ± 0.02
O	16	8	4.08 ± 0.13	4.25 ± 0.13	8.33 ± 0.18	1.04 ± 0.05
F	19	9	4.26 ± 0.13	6.04 ± 0.14	10.3 ± 0.18	1.42 ± 0.05
Al	27	13	6.01 ± 0.20	7.18 ± 0.21	13.2 ± 0.29	1.20 ± 0.05
P	31	15	7.25 ± 0.28	7.54 ± 0.28	14.8 ± 0.4	1.04 ± 0.06
S	32	16	7.76 ± 0.18	6.63 ± 0.16	14.4 ± 0.24	0.85 ± 0.03
K	39	19	9.37 ± 0.42	9.58 ± 0.42	19.0 ± 0.6	1.02 ± 0.1
Ca	40	20	9.01 ± 0.46	5.20 ± 0.46	14.2 ± 0.7	0.58 ± 0.06
Mn	55	25	9.08 ± 0.56	10.9 ± 0.7	20.0 ± 0.9	1.20 ± 0.11
Co	59	27	9.79 ± 0.35	13.1 ± 0.35	22.9 ± 0.5	1.34 ± 0.07
As	75	33	9.72 ± 0.49	13.9 ± 0.7	23.6 ± 0.9	1.43 ± 0.1
I	127	53	15.8 ± 0.7	23.2 ± 0.8	39.0 ± 1.1	1.46 ± 0.08
Bi	209	83	19.2 ± 1.4	25.3 ± 1.4	44.5 ± 2.0	1.32 ± 0.12

The densities of the D, C, O, F, Al, P, S, Ca, I, and Bi targets were adjusted by choosing the mode of subdivision and packing of the material so that the

mean energy loss (~5 Mev) of the escaping pions was roughly the same as that in the water target. The stopping power for pions was too low for Li and K and too high for the Be, Mn, Co, and As. The yields from D, F, Ca, Mn, and As were obtained by a subtraction method. The measured counting rates were corrected for the measured dead-time loss ((~15 percent), the empty target background (~10 percent), and the gamma ray absorption in the target (usually 1 - 3 percent, but reaching 30 percent for Bi).

If pions that are created below the surface of the nucleus have a small escape probability, then one would expect that the sum of the yields per nucleus of both positive and negative pions should be proportional to the surface area of the nucleus. Indeed, because of the observed fluctuations of the negative to positive ratio with mass number, Littauer and Walker obtained a better fit to their data by plotting the sum of the yields of both positive and negative pions vs. the mass number A than by plotting the yield of either the positive or the negative pions alone vs. the mass number A. The total charged pion yield per nucleus is plotted in Figure 9 against the logarithm of the mass number. The known absorption[5] of pions in nuclear matter predict the observed $A^{2/3}$ dependence in the case of the heavier nuclei.

2. <u>The Physical Interpretation</u>

The decrease in the charged pion photoproduction cross sections per nucleon versus the atomic number has been attributed to two causes. Firstly, the exclusion principle limits the volume in phase space available to the residual nucleon so that the cross section per bound nucleon is smaller than the cross section per free nucleon. Secondly, a further decrease is not incompatible

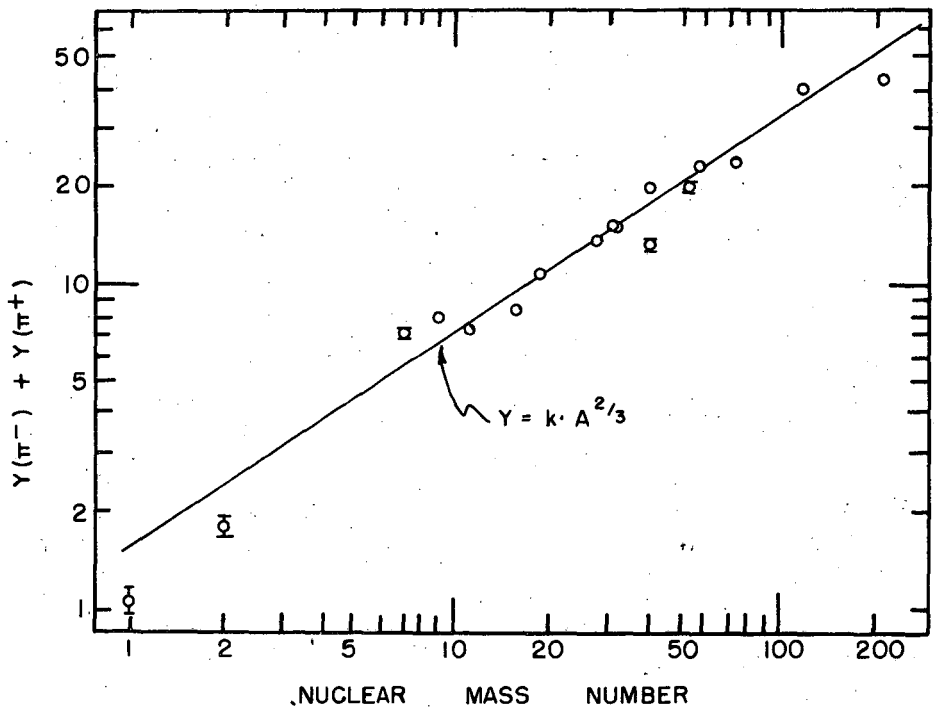
50
20
10
5
2
1
Y(π⁻) + Y(π⁺)
Y = k· A^2/3
1
2
5
10
20
50
100
200
NUCLEAR MASS NUMBER

FIG. 9

MU3911

with the possibility that only the nucleons on the surface of the nucleus take part in photopion production. Since the mean free path for photons in nuclear matter is large compared to the nuclear radius, the decrease in the photopion yield versus Z cannot be explained by "screening" of the internal nucleons from the bombarding γ-rays. If the entire decrease in the cross section per nucleon versus the atomic number is assumed to be due to the absorption of outgoing pions by nucleons, then an upper limit for the mean free path of pions in nuclear matter is calculated[17] to be less than a small multiple of the nuclear radius. This conclusion is in agreement with recent experiments on nuclear interactions of high energy pions. Since the nuclear interaction decreases rapidly with decreasing pion energy, the yield per nucleus of low energy pions might be expected to increase directly as the mass number A of the target nucleus.

III. THE PHOTOPRODUCTION OF NEUTRAL PIONS

A. The γ- γ Coincidence Detection Technique[18]

Steinberger, Panofsky and Steller[18] have developed the gamma-gamma coincidence technique to study the photoproduction of neutral pions. The geometry of the detection apparatus for observing γ- γ coincidences from neutral pion disintegrations is shown in Fig. 10. Each scintillation counter telescope consists of an anti-coincidence phosphor, a positron-electron pair converter of high energy γ-rays, and two coincidence phosphors. An absorber may be introduced between the two coincidence phosphors to measure the energy of the conversion products. A "count" is registered if each of the four coincidence phosphors responds simultaneously (within the resolution time of the apparatus) to a particle of minimum ionization or more and neither of the two anti-coincidence phosphors responds. The arguments for the detection of a neutral pion that decays into two gamma rays are the following:

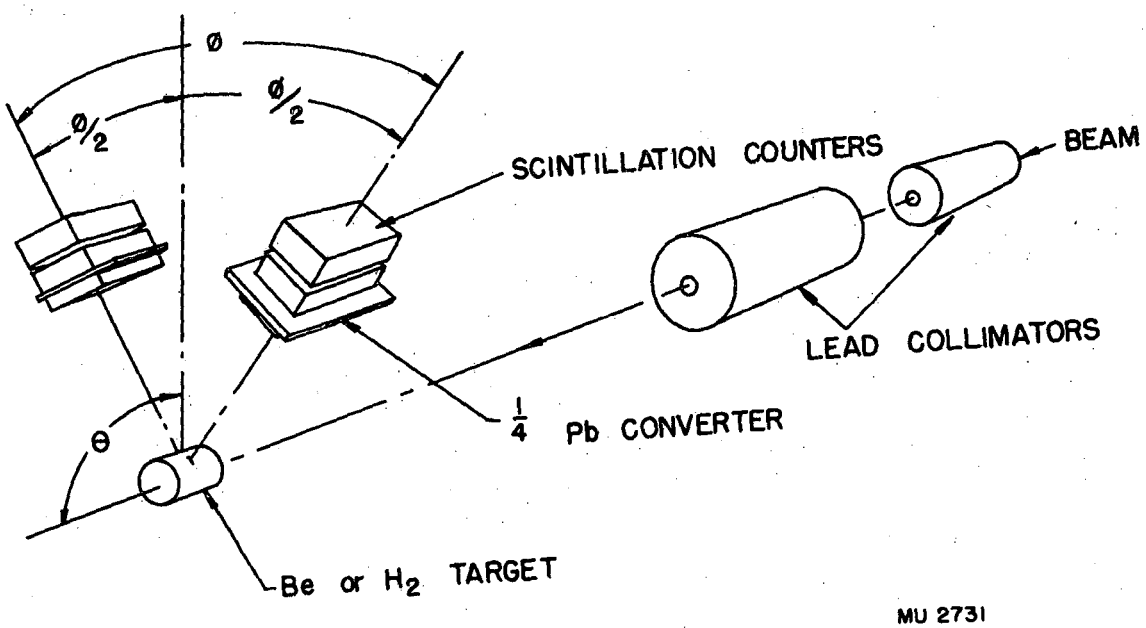
Ø
Ø/2
Ø/2
SCINTILLATION COUNTERS
BEAM
LEAD COLLIMATORS
1/4 Pb CONVERTER
Θ
Be or H2 TARGET
MU 2731

Fig. 10

1. The particles counted in each telescope are non-ionizing initially but are converted into ionizing radiation at the converter.

2. Data on the conversion products as a function of the converter thickness and of the converter material are in agreement with the initial non-ionizing radiation being γ-rays but not neutrons.

3. If the ionizing conversion products are assumed to be pair electrons, then the observed mean electron energy of the more energetic of the pair electrons corresponds to a γ-ray energy that is in good agreement with the kinematics of a π^0, of rest mass of about 135 Mev, disintegrating into two γ-rays.

4. The angular correlation of the photons, notably the existence of a minimum correlation angle ϕ, measured between the two telescope arms, is in agreement with the kinematical relationship appropriate to π^0 disintegration.

B. <u>The Dependence of the Production Cross Section on the Mass Number A or Atomic Number Z</u>

The Z dependence of neutral pion production was studied by measuring the yield of γ-γ coincidences at a correlation angle $\phi = 75^\circ$ and a "yoke" angle $\alpha = 45^\circ$. The "yoke" angle defines the orientation with respect to the beam direction, of the plane containing the two telescopes. The "yoke" refers to the yoke-like mounting arrangement for the two telescopes. The γ-γ coincidence counts as a function of the atomic number Z of the target material are tabulated in Table 4.

TABLE 4

Material	g/cm^2	counts/monitor/nucleon	Number of counts observed
Li	2.71	0.190 ± 0.012	365
Be	8.80	0.148 ± 0.007	458
C	8.09	0.145 ± 0.009	307
Al	1.51	0.126 ± 0.012	129
Cu	0.90	0.077 ± 0.010	74
Pb	0.39	0.051 ± 0.020	20
H		0.208 ± 0.029	

The C and Be targets were solid cylinders; the Li, Al, Cu and Pb targets consisted of these elements inserted in bakelite cylinders. The π^0 yield per nucleon is a decreasing function of Z. Figure 11 shows a log-log plot of the π^0 yield per nucleon and also of the π^+ yield per proton (according to Mozley[12]) versus $A^{-1/3}$. Both sets of data are compatible with a straight line dependence so that the yield is proportional to the nuclear area. Thus, if the decreasing yields versus atomic number result from nuclear absorption of the pions, these data suggest that the mean free path for absorption of neutral pions is approximately the same as that for charged pions.

C. The Disintegration Kinematics of Neutral Pions

Some kinematical relationships of neutral pion decay into two photons aid in interpreting the gamma-gamma coincidence counting rates as a function of the correlation angle ϕ and the yoke angle α.

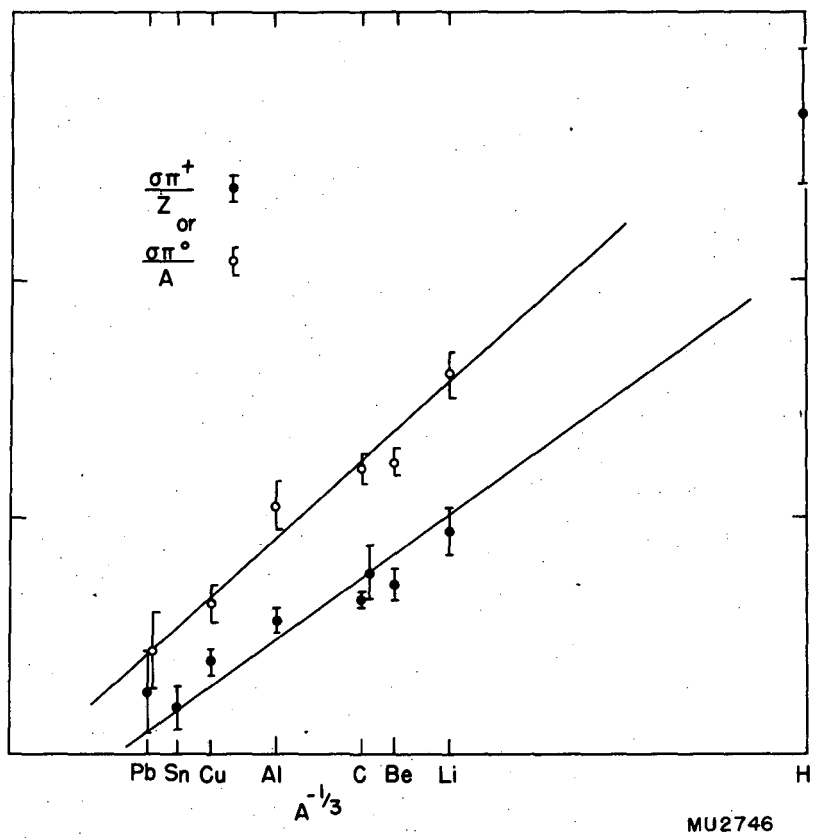
$\frac{\sigma\pi^+}{Z}$
or
$\frac{\sigma\pi^\circ}{A}$
Pb Sn Cu Al C Be Li H
$A^{-1/3}$
MU2746

Fig. 11

The minimum included angle ϕ_{min} between two photons from a neutral pion of a given velocity $\vec{\beta}c$ will occur when the photons are emitted, in the neutral pion rest frame, perpendicular to the direction of motion of the neutral pion. Hence, from the geometry of Fig. 12, we can write immediately $\cos \frac{\phi_{min}}{2} = \beta$

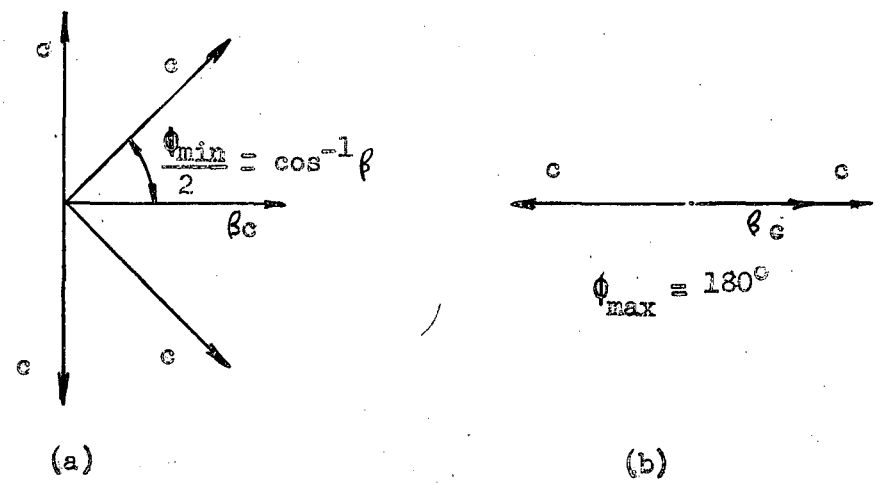

Fig. 12

Figure 13 shows a plot of ϕ_{min} versus the neutral pion kinetic energy in units of the rest mass of the neutral pion. Note the qualitative feature that larger neutral pion energies are associated with smaller values of the minimum correlation angle ϕ.

If the decay photons are emitted isotropically in the neutral pion rest frame, then the calculated probability $P(\phi)\, d\phi$ of observing a given included angle ϕ in the interval $d\phi$ from neutral pions of velocity β (which is functionally related to ϕ) is

$$P(\phi)\, d\phi = \sin \phi \frac{1}{(1 - \cos \phi)^{3/2}} \frac{(1 - B^2)\, d\phi}{\beta\,(2\beta^2 - 1 - \cos \phi)^{1/2}}$$

This correlation function is shown (Fig. 14) plotted against ϕ for three values of β corresponding to neutral pion kinetic energies of 20, 60 and 100 Mev. Note that the probability for any given value of β is largest near the minimum correlation angle ϕ_{min} for that β. Hence, an approximate one-to-one correspondence exists between the observed correlation angles and the neutral pion

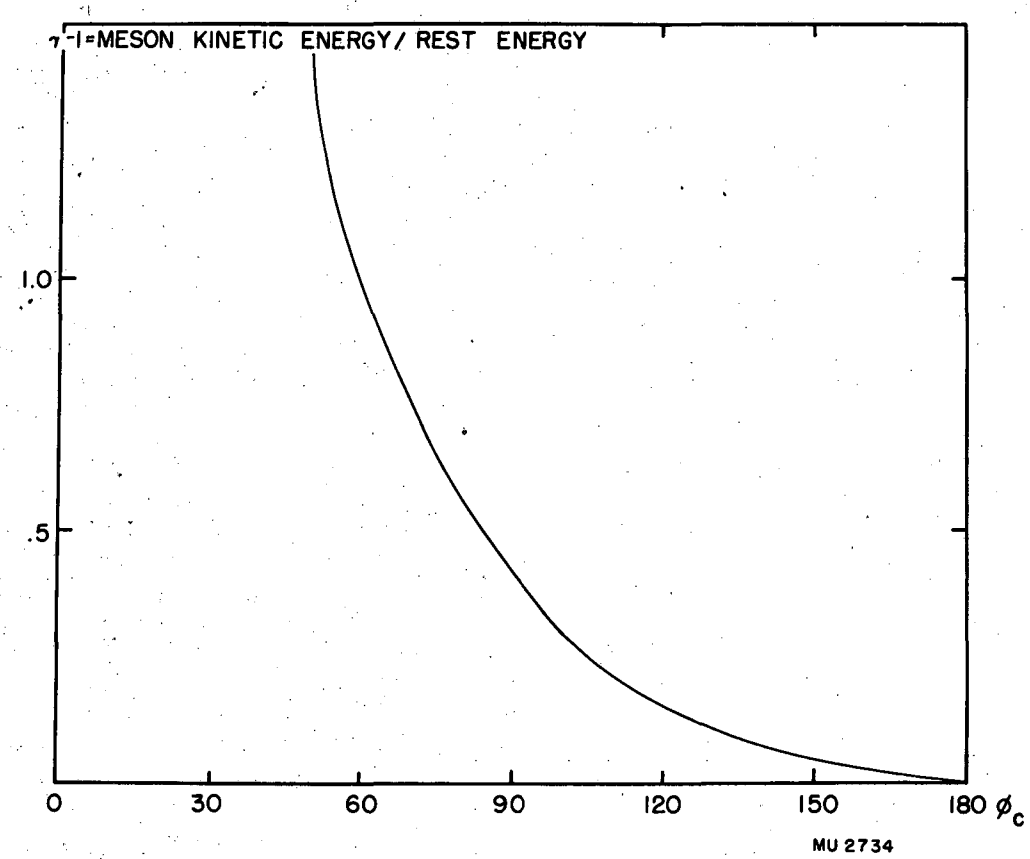
γ-1=MESON KINETIC ENERGY/ REST ENERGY
1.0
.5
0
30
60
90
120
150
180 ϕ_c
MU 2734

Fig. 13

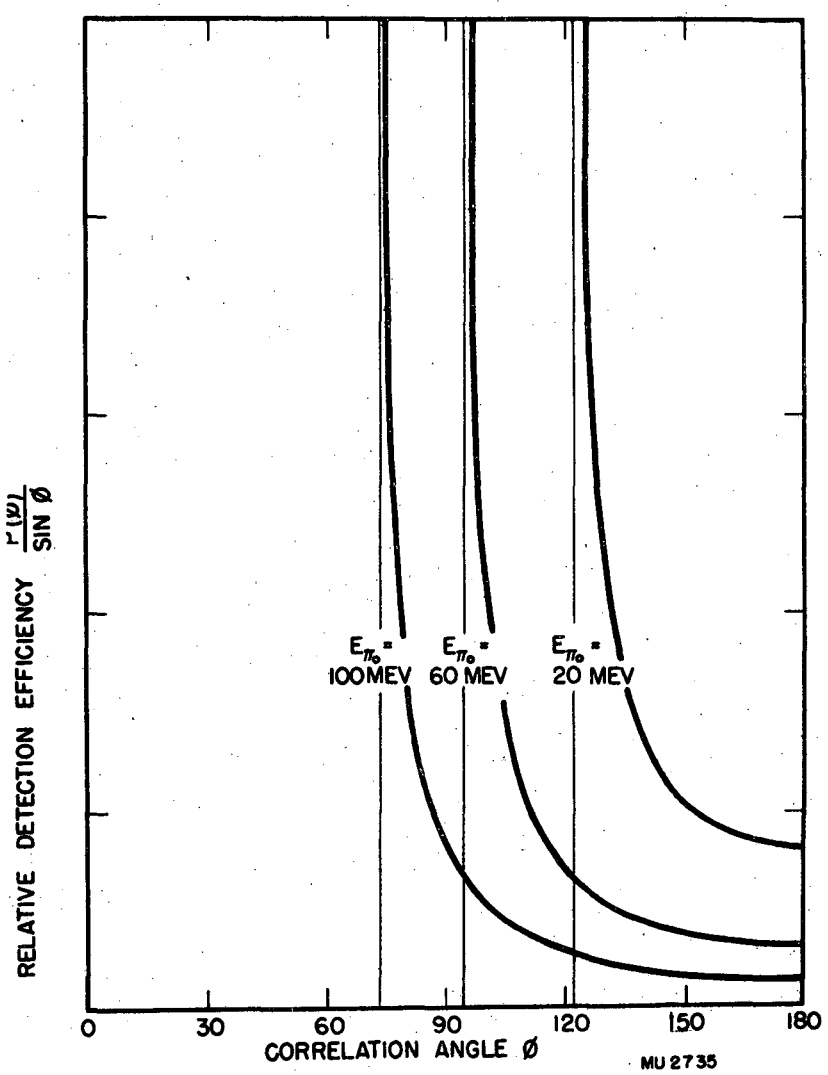
RELATIVE DETECTION EFFICIENCY $\frac{r(\phi)}{\sin \phi}$
E_{π_0} = 100 MEV
E_{π_0} = 60 MEV
E_{π_0} = 20 MEV
0
30
60
90
120
150
180
CORRELATION ANGLE Ø
MU 2735

Fig. 14

velocity. The detection efficiency of the experimental arrangement further emphasizes this one-to-one correspondnece; the reason is that, for a given neutral pion velocity, both γ rays will have high energy and thus be detected efficiently near $\phi \approx \phi_{min}$, whereas one of the two γ-rays will have low energy near $\phi \approx 180^{\circ}$. This discriminatory effect on the energy spectrum of the neutral pions is greater for the high energy end of the π^{o} spectrum. The lowest neutral pion energy that can produce photons at a given correlation angle ϕ is determined by the relation

$$\gamma_{min} \equiv \frac{E_{min}}{E_o} \equiv \frac{1}{(1-\beta^2_{min})^{1/2}} = \csc \frac{\phi}{2}$$

or

$$\beta_{min} = \cos \frac{\phi}{2}$$

D. The Photoproduction of Neutral Pions from Beryllium

1. The Observed Angular Correlation

Figure 15 shows the relative coincidence counting rates from a beryllium target as a function of the correlation angle ϕ for three values of the yoke angle $\theta = 45^{\circ}$, 90°, and 135°. The qualitative features of the kinematics of neutral pion disintegration into two photons is confirmed by these spectra. Note that the minimum correlation angle decreases with forward yoke angles because the upper limit of neutral pion energy increases.

2. The Approximate Evaluation of the Energy Distribution of the Neutral Pions

The energy distributions shown in the first paper by Steinberger, Panofsky and Steller[18] have been evaluated from the observed angular correlation curves by assuming that the energy γ (= E/E_o) of the neutral pions at a given correlation angle ϕ is given by the median correlation angle, viz.

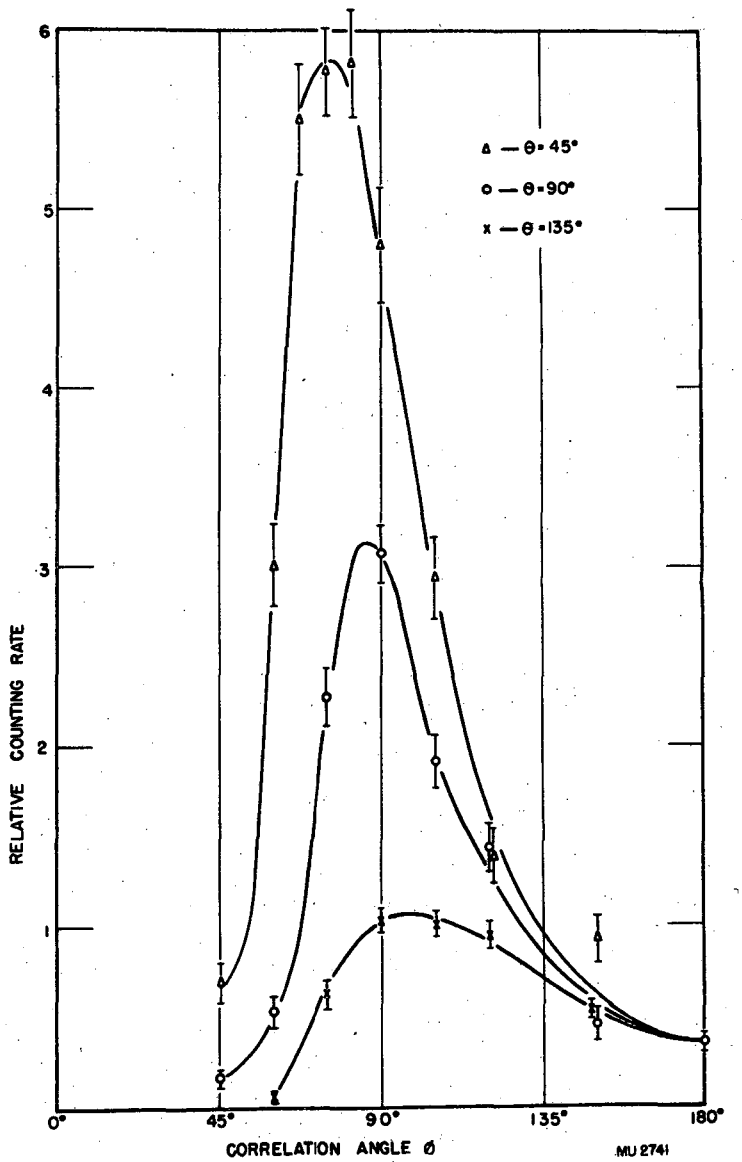
6
5
4
3
2
1
RELATIVE COUNTING RATE
Δ — θ = 45°
o — θ = 90°
x — θ = 135°
0°
45°
90°
135°
180°
CORRELATION ANGLE Ø
MU 2741

Fig. 15

$$\phi_{median} = 2 \sin^{-1} \frac{2}{(3\gamma^2 + 1)^{1/2}}$$

The fact that neutral pions of a given energy are concentrated heavily within a small range of correlation angles is illustrated once more by the following example. For 70 Mev neutral pions, the minimum correlation angle is 84°; the median correlation angle is 92°. The energy distribution at yoke angles of 45° and 135° were evaluated by making the further assumption that the production angles do not deviate very much from the yoke angle. The basis for this assumption is the near one-to-one correspondence between the observed correlation angle and the neutral pion velocity. A yoke angle of 90° collects γ-γ coincidence counts from neutral pions emitted always at production angles of 90°; a yoke angle other than 90° collects γ-γ coincidence counts from neutral pions emitted over a distribution of production angles for a distribution of neutral pion velocities.

The energy distribution of the neutral pions appears in the integrand of an integral equation for the γ-γ coincidence counting rate. This integral equation has been written down and inverted exactly[19] by formal methods for a yoke angle of 90°. Exact inversion has not been accomplished at a more general yoke angle chiefly because of the complicated relations introduced by the more general geometry. If $N_\gamma(\phi, \alpha)\, d\phi\, d\alpha$ represents the observed γ-γ coincidence counting rate at a correlation angle ϕ in the range $d\phi$ and at a yoke angle α in the range $d\alpha$, then since $\alpha = \theta = \frac{\pi}{2}$,

$$N_\gamma(\phi, \tfrac{\pi}{2})\, d\phi = 2 \int_{E_{min}}^{E_{max}} P(\phi)\, d\phi \frac{d\sigma(E, \pi/2)}{dE\, d\Omega}\, dE \left(\frac{\Delta\Omega_1}{4\pi} \; \frac{\Delta\Omega_2}{2\pi \sin\phi\, d\phi} \right)$$

where $\frac{d\sigma(E, \pi/2)}{dE\, d\Omega}$ is the spectral differential cross section per equivalent photon and per target atom for production of neutral pions at a laboratory angle of 90° and at a laboratory energy E in the range dE.

$\Delta\Omega$, and $\Delta\Omega_2$ are the solid angles subtended at the production targets by the limiting aperture of each telescope.

The factor $\frac{\Delta\Omega_2}{2\pi \sin\phi \, d\phi}$ gives the probability of catching the second γ-ray in the second telescope, after having already caught the first γ-ray in the first telescope.

The factor 2 appears because the photons are indistinguishable, that is, either γ-ray can be caught in the first telescope.

E_{max} is the energetic upper limit of the production process.

E_{min} is the lowest neutral pion energy that can produce γ-γ coincidences at a correlation angle ϕ. We wrote down previously that $E_{min} = E_o \csc \frac{\phi}{2}$.

For the purposes of "unfolding" the energy distribution, note that the integral to be inverted has the form

$$C(\phi) \sim \int \frac{d\sigma}{d\Omega dE} \pi(\phi, E)\, dE \rightarrow \sum_{i=1}^{N} A_i \, \pi_i^N (\phi, E) \Delta E_i$$

Panofsky et al[18] fitted the observed angular correlation curve for $\theta = 90^o$ by a finite number N of step functions and "synthesized" a step function energy distribution as follows:

Since $C^N \sim \sum_{i=1}^{N} A_i \, \pi_i^N (\phi^N, E_i) \Delta E_i$, the N arbitrary amplitudes A_i are obtained by fitting the observed angular correlation curve at N points and solving N simultaneous linear equations. This analysis is illustrated in Fig. 16. For example, picking a value ϕ^N determines C^N. Then, by also choosing a value of E_i, $\pi_i^N (\phi^N, E_i)$ is determined.

Fig. 16

Figure 17 shows the energy distribution of neutral pions that would give rise to the observed γ-γ coincidence correlation curve for a yoke angle of 90° from a beryllium target. The fit is made with six "square step" distributions of suitably adjusted amplitude.

Figure 18 shows a comparison of the observed correlation data with the curve calculated on the basis of the "square step" energy distribution of Fig. 17. The observed correlation curves are not very sensitive to details in their energy distribution, but they are sufficiently sensitive to give the relative amounts of low energy and high energy contributions in the distribution. The reason is that each high energy component will contribute intensity between the corresponding lower limiting correlation angle and 180°. Hence, if the high energy components already account for the entire intensity at $\phi = 180°$, then very little low energy components can be present. The synthesized energy distirbution shows that this is the case for π^0's from Be. Figure 19 shows in contrast the expected correlation curve if the π^0 energy distribution had been identical with the π^+ spectrum photoproduced from H at 90°[14].

3. <u>The Absolute Cross Sections and the Angular Distribution of Neutral Pions from Beryllium</u>

The absolute cross sections per effective quantum are directly obtainable by numerical integration of the observed angular correlation data. The published results are:

θ	$\frac{d\sigma}{d\Omega}(\theta)$
45°	4.41×10^{-29} cm^2/effective quantum/steradian
90°	3.13
135°	1.06

$$\sigma = \int \frac{d\sigma}{d\Omega}\, d\Omega = 3.7 \times 10^{-28} \text{ cm}^2/\text{effecitve quantum}$$

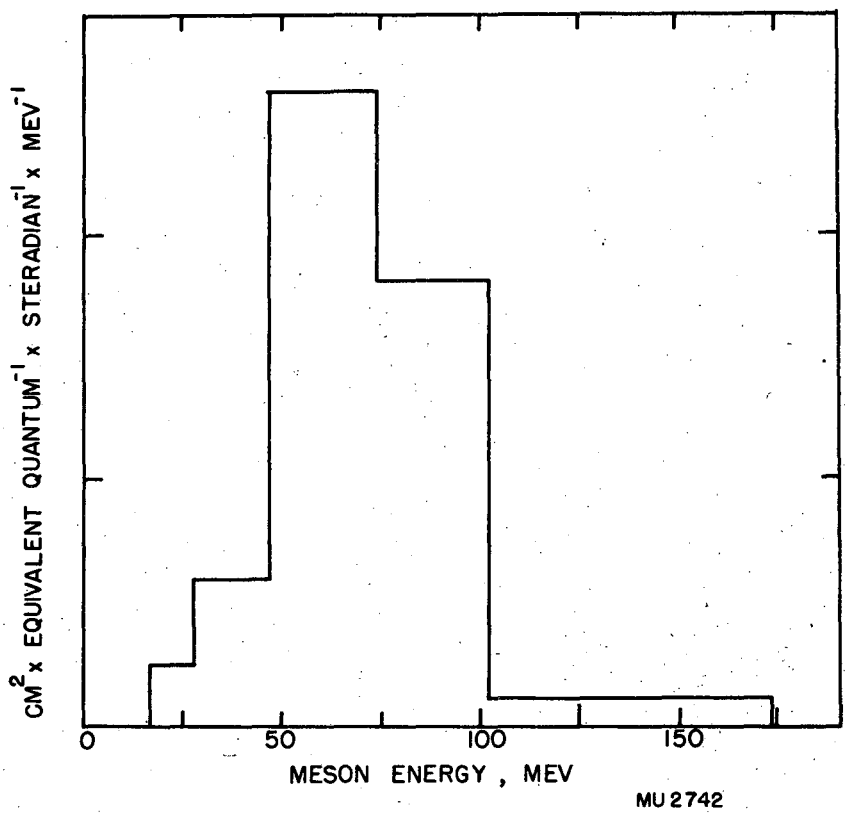
CM^2 x EQUIVALENT QUANTUM^{-1} x STERADIAN^{-1} x MEV^{-1}
0
50
100
150
MESON ENERGY , MEV
MU 2742

Fig. 17

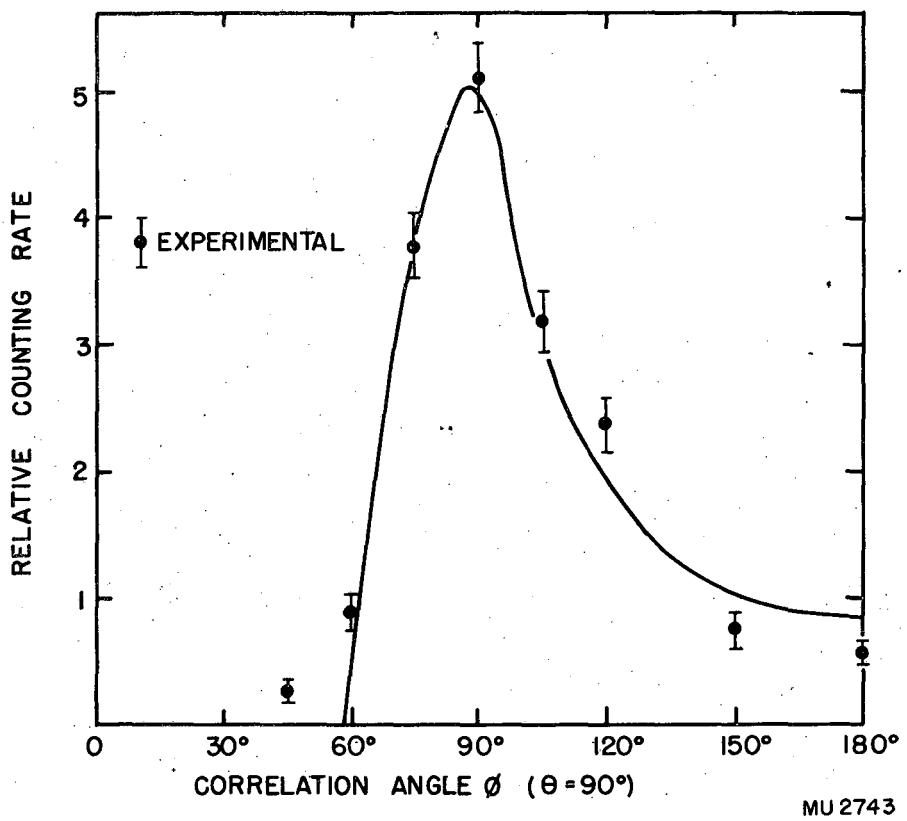
EXPERIMENTAL
RELATIVE COUNTING RATE
5
4
3
2
1
0
30°
60°
90°
120°
150°
180°
CORRELATION ANGLE Ø (θ = 90°)
MU 2743

Fig. 18

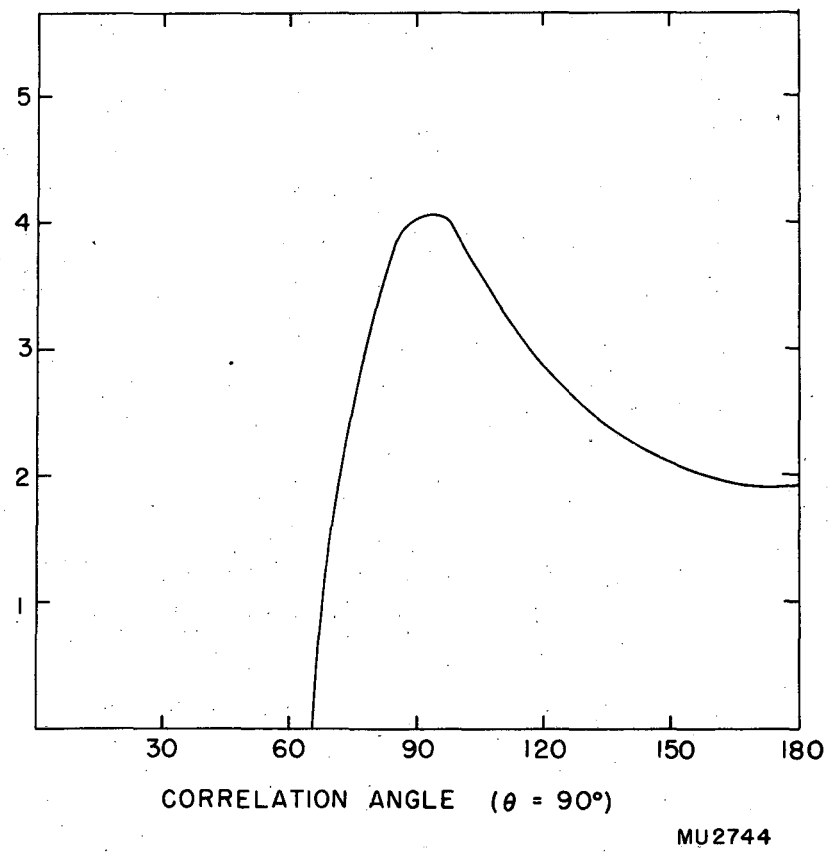

Fig. 19

True absolute cross sedtions per photon at a definite photon energy can be derived from observed data in the following approximations.

a. The production kinematies of a neutral pion that is photo-produced from a Be nucleus is the same as that from a free nucleon. That is, a unique relationship is assumed between the neutral pion energy, at production, and the primary photon bombarding energy.

b. The one-to-one correspondence between the correlation angle ϕ and the neutral pion velocity is exact. That is, the calculated angular correlation curves are assumed to be delta functions located at a mean correlation angle; hence, the "yoke" angle α is taken equal to the production angle θ for "yoke" angles different from 90°.

c. The number of quanta in a primary x-ray energy interval dk of the bremsstrahlung spectrum from the synchrotron is given very closely by $dQ = Q\, dk/k$.

The correlation angle was adjusted at each production angle to correspond to the production of neutral pions from 260 Mev photons. The differential cross sections, calculated in these approximations from the observed data, are given in Table 5.

TABLE 5

Angular distribution of π^0 photoproduction in beryllium

(The zero subscripts refer to quantities in the center of mass coordinate system)

ϕ	ϵ	θ_o	$\frac{d\sigma}{d\Omega}$ (k = 260 Mev) x 10^{29} cm^2/steradian	$\frac{d\sigma}{d\Omega_o}$ x 10^{-29} cm^2/steradian
70°	34°	44°	4.66 ± 0.27	2.35 ± 0.14
75°	45°	57 1/2°	7.64 ± 0.36	4.52 ± 0.22
80°	55°	69°	6.69 ± 0.33	4.52 ± 0.22
82 1/2°	67 1/2°	83°	7.36 ± 0.37	5.90 ± 0.30
90°	90°	106°	5.62 ± 0.26	6.33 ± 0.29
97 1/2°	112°	126°	3.00 ± 0.22	4.53 ± 0.33
105°	135°	145°	1.35 ± 0.10	2.52 ± 0.21
115°	150°	157°	0.676± 0.08	1.42 ± 0.17

The integrated neutral pion production cross section for 260 Mev photons is 5.55 x 10^{-28} cm^2 per beryllium nucleus. (The integrated positive pion production cross section for 255 Mev photons is 1.9 ± 0.3 x 10^{-28} cm^2 per hydrogen nucleus). The fact that the total cross section per 260 Mev photon is almost twice as large as the value (3.7 x 10^{-28} cm^2) quoted per effective quantum is reasonable since the excitation function rises slowly near threshold.

The authors claim that the quoted absolute values should be accurate to a factor of two; however, three significant figures are given to permit internal comparison. Probable errors refer to statistics only.

Figure 16 is a plot of the absolute cross section per 260 Mev photon for neutral pion production from Be as a function of the laboratory production

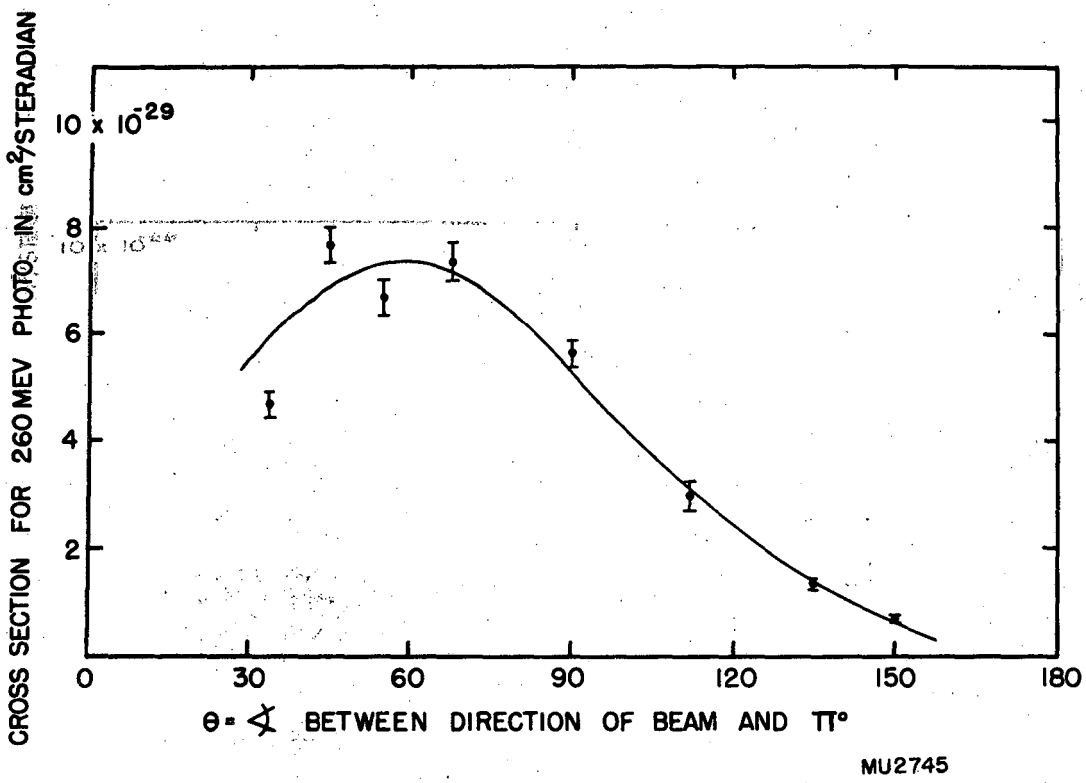
CROSS SECTION FOR 260 MEV PHOTONS IN cm²/STERADIAN
10 x 10⁻²⁹
8
6
4
2
0
30
60
90
120
150
180
θ = ∢ BETWEEN DIRECTION OF BEAM AND TT°
MU2745

Fig. 20

angle. This result, based on the above analysis, indicates that the angular distribution for the photoproduction of neutral pions from photons of a given energy is strongly peaked forward in the laboratory coordinate system.

If this angular distribution is transformed to the center of mass coordinate system, then the result* is shown in Fig. 21. The positive pion angular distribution from hydrogen is plotted also for comparison.

Three effects would make the angular distribution of neutral pions from a beryllium nucleus differ from that from a free proton.

a. The Be cross section includes production both from protons and neutrons.

b. The internal motion of the nucleons in Be would favor the production of neutral pions from nucleons that are moving toward the bombarding photons because of the steep excitation function for the neutral pion photoproduction process.

c. The exclusion principle could introduce a modification because the energy available to the recoil nucleon is a function of the neutral pion production angle.

E. <u>The Photoproduction of Neutral Pions from Hydrogen (Preliminary Data)</u>

1. <u>The Cross Sections</u>

a. The Polyethylene (CH_2) - Carbon Subtraction Method

No data were taken on either the correlation function or the angular distribution because adequate statistics were difficult to obtain

---

* The calculation of the center of mass angular distribution from the laboratory angular distribution was accomplished by assuming that the kinematics of the reaction $\gamma + p \rightarrow \pi^0 + p$ is the same as the kinematics for the reaction $\gamma + n \rightarrow \pi^- + p$. This assumption was made for convenience because the kinematics of the latter reaction had already been calculated in detail[20].

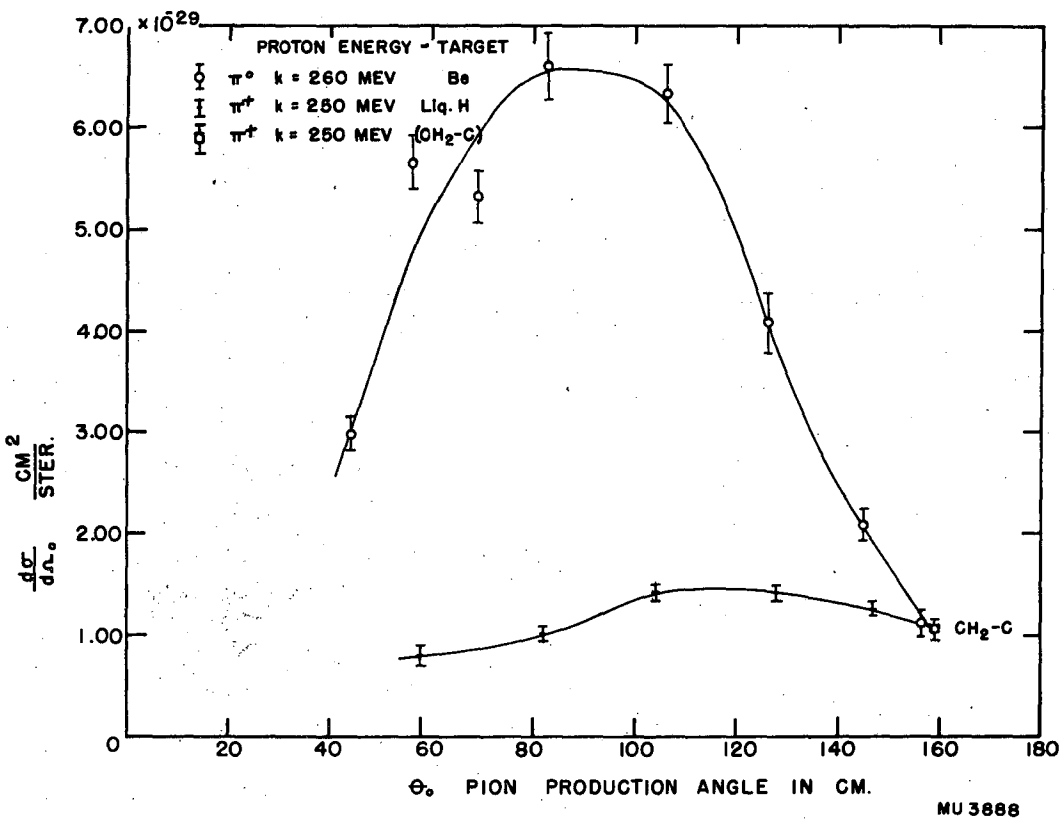
PROTON ENERGY - TARGET
π° k = 260 MEV Be
π+ k = 250 MEV Liq. H
π+ k = 250 MEV (CH2-C)
CH2-C
7.00 x 10^-29
6.00
5.00
4.00
3.00
2.00
1.00
0
20
40
60
80
100
120
140
160
180
dσ/dΩ₀ CM²/STER.
θ₀ PION PRODUCTION ANGLE IN CM.
MU 3888

Fig. 21

with the subtraction method; however, data were observed at the correlation angle of 90° and at the yoke angle of 90°. These data give the result that

$$\frac{\sigma_H}{\sigma_C} = 0.120 \pm 0.025$$

If the correlation functions for hydrogen and beryllium are assumed to be similar, then the total cross section for neutral pion photoproduction from hydrogen is estimated to be

$$\sigma = 0.60 \times 10^{-28} \text{ cm}^2/\text{effective quantum at 320 Mev.}$$

b. The Production from Liquid Hydrogen

Figure 22 shows some preliminary angular correlation data for the photoproduction of neutral pions from liquid hydrogen at a production angle of 90°. Angular correlation data were also taken at a yoke angle of 45°. Note that the observed angular correlation from hydrogen is very similar to that from beryllium. Absolute cross sections were estimated from these data to be

$$\left.\frac{d\sigma}{d\Omega}\right|_{\theta = 90^\circ} = 3.5 \times 10^{-30} \text{ cm}^2/\text{steradian/effective quantum}$$

$$\left.\frac{d\sigma}{d\Omega}\right|_{\theta = 45^\circ} = 8.2 \times 10^{-30} \text{ cm}^2/\text{ steradian/ effective quantum}$$

$$\sigma = 0.55 \times 10^{-28} \text{ cm}^2/\text{effective quantum.}$$

The total cross section is in good agreement with the result derived from the subtraction method.

A correction factor of 0.70 ± 0.05 was applied to the raw data from liquid hydrogen because the empty target background averaged 30 ± 5 percent, and statistics were insufficient to justify a point-by-point correction of the observed data.

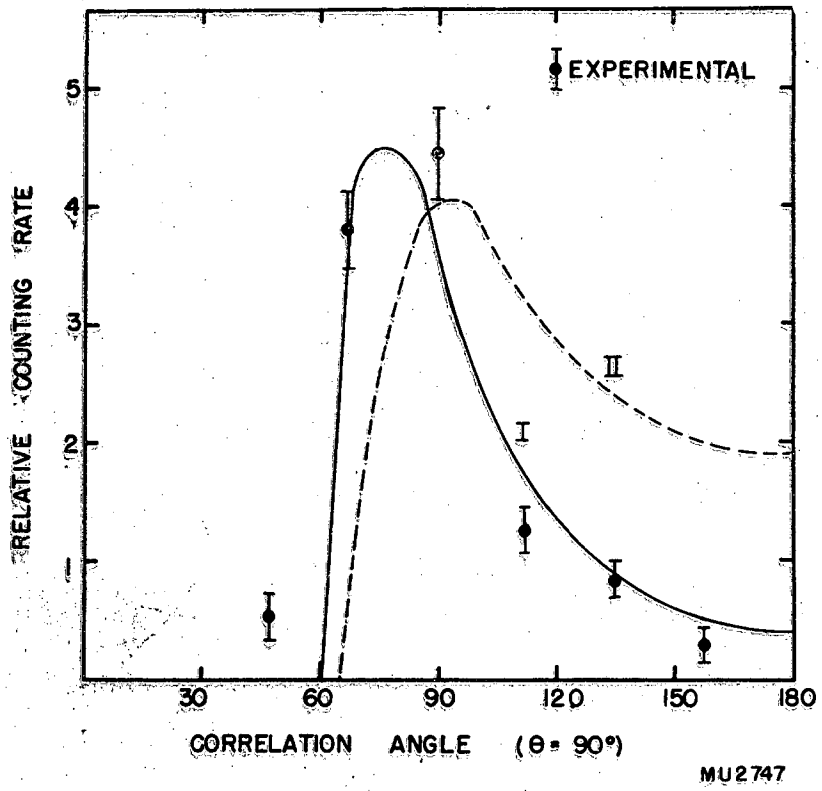
EXPERIMENTAL
RELATIVE COUNTING RATE
5
4
3
2
1
II
I
30
60
90
120
150
180
CORRELATION ANGLE (θ = 90°)
MU2747

Fig. 22

2. The Excitation Function

Figure 23 is a step function energy spectrum that is compatible with the observed gamma-gamma coincidence angular correlation from neutral pion photoproduction at 90°. This four step energy distribution was synthesized for the hydrogen data in the same manner as that for the beryllium data.

The solid curve on Fig. 22 is the expected correlation curve if the spectrum were this synthesized four step spectrum. The dotted curve is the expected correlation curve if neutral and positive photopion production were identical.

This analysis of the observed angular correlation curve from liquid hydrogen leads to the conclusion that the excitation function for the photoproduction of neutral pions has a higher order contact near threshold than that for positive pions. This conclusion, that the neutral pion photo excitation curve starts more slowly from threshold than the positive pion photo excitation curve, has been verified independently by the experiment of Silverman and Stearns[21] at Cornell.

F. The Photoproduction of Neutral Pions from Hydrogen

1. The Experimental Technique

Silverman and Stearns[21] at Cornell observed the reaction $\gamma + p \rightarrow \pi^0 + p$ by detecting coincidences between the recoil proton and one of the decay photons from the neutral pion. The experimental arrangement is shown schematically in Fig. 24. The recoil protons come to rest in a NaI phosphor, which is located at 30° ± 3° to the beam; the pulse height in the proton detector is a measure of the proton energy. The γ-ray detector consists of an anticoincidence phosphor, a positron-electron pair converter of high energy gamma rays, and two coincidence phosphors. For a proton angle of 30°, the correlated neutral pion angle is 90° ± 10° for incident photons between 200 Mev and 310 Mev; hence the γ-ray detector was set at 90° with an angular aperture of ± 5°. The γ-ray counter was placed in the direction of emission of

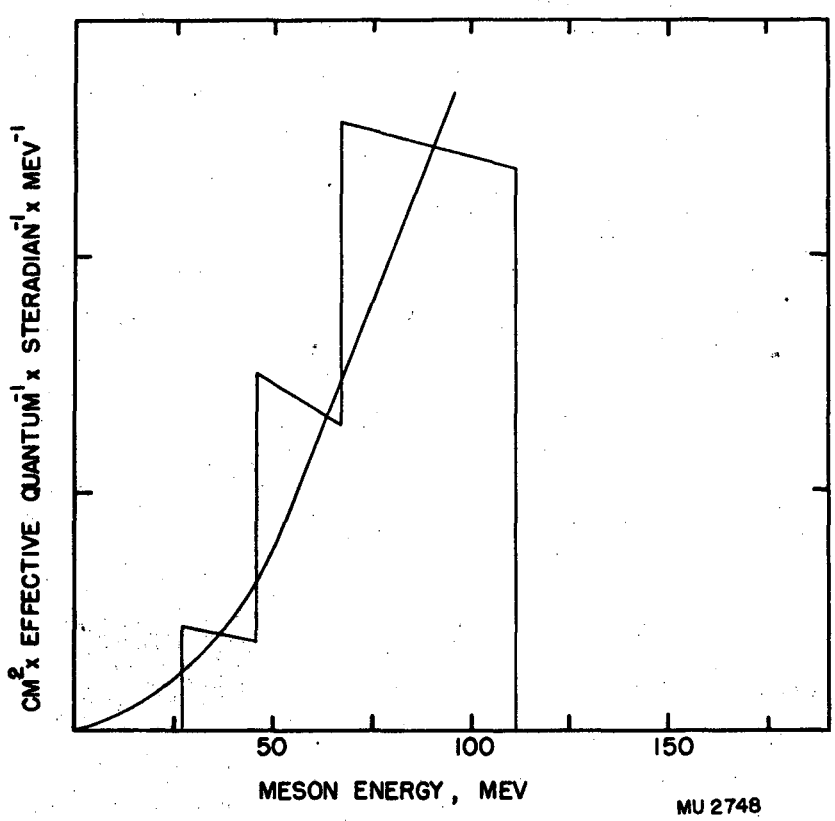
CM^2 x EFFECTIVE QUANTUM^{-1} x STERADIAN^{-1} x MEV^{-1}
50
100
150
MESON ENERGY, MEV
MU 2748

Fig. 23

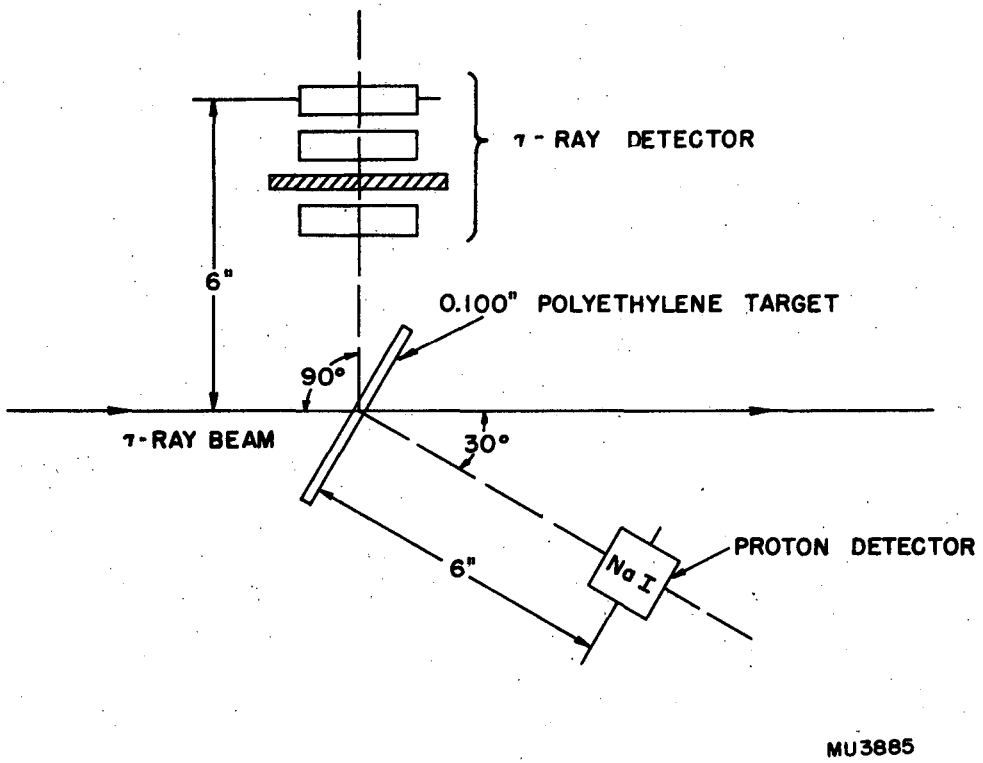
γ - RAY DETECTOR
6"
0.100" POLYETHYLENE TARGET
90°
γ-RAY BEAM
30°
6"
NaI
PROTON DETECTOR
MU3885

Fig. 24

the neutral pion for maximum efficiency. Very thin polyethylene (CH_2) and carbon targets were required in order to prevent excessive degradation of the energy of the recoil protons in the target. The CH_2 target was 0.23 g/cm^2 (0.100 in.) thick; the thickness of the carbon target was chosen to provide equal stopping power for protons.

2. The Excitation Function and the Cross Section

The measurements of the energy and the angle of the recoil proton are sufficient to uniquely determine the kinematics of this reaction. The cross section for neutral pion production at 90° in the laboratory system as a function of the incident gamma ray energy is shown in Fig. 25. The indicated errors include estimated instrumental as well as statistical errors. The data can be fitted by the power law

$$\frac{d\sigma}{d\Omega} \sim (k - \mu)^{1.8 \pm 0.5}$$

where k = the bombarding photon energy, and

μ = the rest mass of the neutral pion.

The curvature of the neutral pion excitation function is in sharp contrast with the curvature of the positive pion excitation function. The data of Steinberger and Bishop can be approximated very crudely by $\frac{d\sigma}{d\Omega} \sim (k - \mu)^{0.5}$. The absolute magnitudes of the two cross sections are roughly the same at a bombarding energy of 300 Mev.

3. The Angular Distribution

The ratio of the differential cross sections at the laboratory production angles of 60° and 90° for photons from 250 Mev to 310 Mev is

$$\frac{\left(\frac{d\sigma}{d\Omega}\right)_{\theta = 60^\circ}}{\left(\frac{d\sigma}{d\Omega}\right)_{\theta = 90^\circ}} = 1.50 \pm 0.25;$$

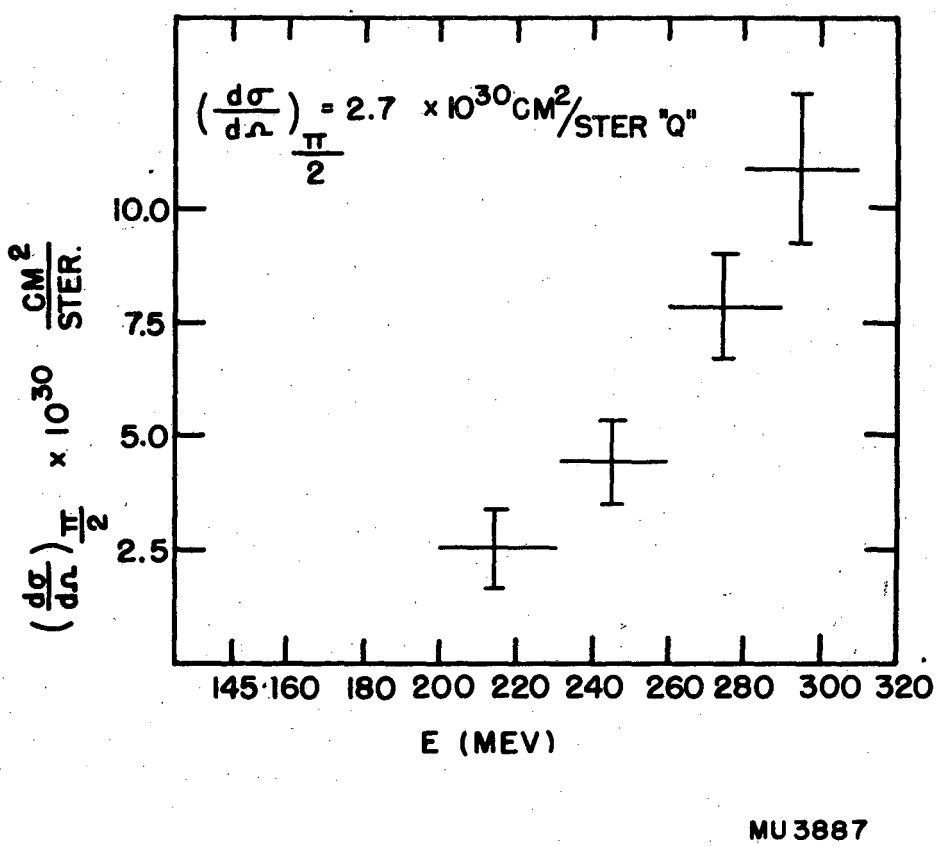

MU 3887

Fig. 25

the ratio of the differential cross sections at the corresponding center of mass production angles of 76° and 112° is

$$\frac{\left(\frac{d\sigma}{d\Omega}\right)_{\theta_0 = 76^\circ}}{\left(\frac{d\sigma}{d\Omega}\right)_{\theta_0 = 112^\circ}} = 1.10 \pm 0.20$$

ACKNOWLEDGEMENTS

I would like to thank the members of the theoretical group at the Radiation Laboratory for their interest. In addition, I wish to express my appreciation to Dr. J. V. Lepore and to Dr. M. Ruderman for helpful comments. This paper was prepared under the auspices of the Atomic Energy Commission.

Information Division
7/1/52 bw

REFERENCES

1. E. M. McMillan and J. M. Peterson. Science 109, 438 (1949)
2. R. S. White, M. J. Jakobson, and A. G. Schulz. UCRL-1319 Rev.
3. R. M. Littauer and D. Walker. Phys. Rev. 82, 746L (1951) ; 86, 838 (1952)
4. M. Camac. Rev. Sci. Instr. 22, 197 (1951)
5. H. A. Bethe and R. R. Wilson. Phys. Rev. 83, 690 (1951)
6. K. Brueckner and M. Goldberger. Phys. Rev. 76, 1725 (1949)
7. K. Breuckner. Phys. Rev. 79, 641 (1950)
8. E. M. McMillan, J. Peterson and R. S. White. Science 110, 580 (1949); J. Peterson, W. Gilbert and R. S. White. Phys. Rev. 81, 1003 (1950)
9. M. K. Jakobson. UCRL-1317
10. S. Machida and T. Tamura. Progress of Theoretical Physics, 6, 1030L (1951)
11. H. A. Medicus. Phys. Rev. 83, 662 (1951)
12. J. Carothers. UCRL-1829
13. R. Mozley. Phys. Rev. 80, 493 (1950); UCRL-706
14. J. Steinberger and A. S. Bishop. Phys. Rev. 86, 171 (1952); Phys. Rev. 78, 493 (1950); Phys. Rev. 78, 494 (1950); Bishop. UCRL-874; Bishop, Steinberger and Cook, Phys. Rev. 80, 291 (1950)
15. H. Feshback and M. Lax. Phys. Rev. 76, 134 (1949); G. Chew and H. Lewis, Phys. Rev. 84, 779 (1951)
16. W. Blocker, R. W. Kenney, and W. K. H. Panofsky. Phys. Rev. 79, 419 (1950)
17. K. Breuckner, R. Serber and K. Watson. UCRL-1358
18. J. Steinberger, W. K. H. Panofsky, and J. Steller. Phys. Rev. 78, 802 (1950) Panofsky, Steinberger and Steller. Phys. Rev. 86, 180 (1952); UCRL-1495
19. E. Vaughan, Private Communication
20. R. Madey. UCRL-1634
21. A. Silverman and M. Stearns. Phys. Rev. 83, 206A and 853L (1951)

ILLUSTRATIONS

Fig. 1 The negative to positive ratio of the production cross sections versus the nuclear mass number of the target nucleus.

Fig. 2 The negative to positive ratio of the production cross sections and the mass differences of the ground states of the isobars adjacent in atomic number to the target nucleus versus the atomic number of the target nucleus.

Fig. 3 The negative to positive ratio of the production cross sections versus the mass difference of the ground states of the isobars adjacent in atomic number to the target nucleus.

Fig. 4 Angular distribution for the production of positive pions by 255 Mev photons on hydrogen.

Fig. 5 Energy distribution of positive pions produced at 90° by 325 Mev maximum energy bremsstrahlung on carbon and on hydrogen by subtraction.

Fig. 6 Energy distribution of positive pions produced at 90° by 325 Mev maximum energy bremsstrahlung on a liquid hydrogen target. The solid curve represents the number of photons per unit pion energy, viz. $\frac{dN}{dk} \frac{dk}{dE}$.

Fig. 7 Independent particle model of the C^{12} nucleus.

Fig. 8 Excitation function for the production of positive pions by photons on hydrogen at 90° to the beam.

Fig. 9 The total charged pion yield per nucleus versus the logarithm of the mass number of the target nucleus.

Fig. 10 Geometry of the detection apparatus for observing gamma-gamma coincidences from neutral pion disintegrations. The "correlation angle" φ and the "telescope plane angle" or "yoke angle" θ (approximately the neutral pion production angle) are indicated.

Fig. 11 Cross section of neutral pion production per nucleon and cross section of positive pion production per proton plotted against $A^{-1/3}$, where A is the mass number.

Fig. 12 Disintegration of a neutral pion into two gamma rays (a) transverse and (b) parallel to the neutral pion velocity vector.

Fig. 13 Plot of the neutral pion kinetic energy in units of the rest mass of the neutral pion versus the minimum correlation angle ϕ_{min}.

Fig. 14 Plot of $\frac{P(\varphi)}{\sin\varphi}$ against the correlation angle φ for three values of the neutral pion kinetic energy. This function is the relative detection probability for a given correlated γ ray pair.

Fig. 15 The relative gamma-gamma coincidence counting rates from a berrylium target as a function of the correlation angle φ for three values of the telescope plane angle θ.

Fig. 16 Illustration of the method of synthesizing a step function energy distribution from an experimental gamma-gamma coincidence correlation curve.

Fig. 17 An energy distribution of neutral pions that would give rise to the observed gamma-gamma coincidence correlation curve for a production angle of 90° from a beryllium target. The fit is made with six "square step" distributions of suitably adjusted amplitude.

Fig. 18 A comparison of the observed angular correlation data with the curve calculated on the basis of the "square step" energy distribution of Fig. 13.

Fig. 19 The correlation curve expected if the neutral pion energy distribution from beryllium at 90° had been identical with the positive pion spectrum photoproduced from hydrogen at 90° (as observed by Steinberger and Bishop[13]).

Fig. 20 The absolute cross section per 260 Mev photon for neutral pion production from a beryllium target as a function of the laboratory production angle.

Fig. 21 The center of mass angular distribution for the photoproduction of neutral pions from beryllium. The positive pion angular distribution, in the center of mass, from hydrogen is plotted also for comparison.

Fig. 22 Some preliminary angular correlation data for the photoproduction of neutral pions at a production angle of 90° from liquid hydrogen. The solid curve is the expected correlation curve if the spectrum were the synthesized four step spectrum of Fig. 19. The dotted curve is the expected correlation curve if neutral and positive photopion production spectra were identical.

Fig. 23 A step-energy spectrum that is compatible with the observed gamma-gamma coincidence angular correlation from neutral pion photoproduction at 90°.

Fig. 24 The experimental arrangement for detection of neutral pion-proton coincidences produced by photons on protons.

Fig. 25 The cross section for neutral pion production from hydrogen at 90° in the laboratory system as a function of the incident gamma ray energy.